



Yulieth Alzate Cardona

**Object-based Modeling of Turbidite Lobes using
Single-valued B-Splines**

DISSERTAÇÃO DE MESTRADO

Dissertation presented to the Programa de Pós-graduação em Matemática of the Departamento de Matemática, PUC-Rio as partial fulfillment of the requirements for the degree of Mestre em Matemática.

Advisor: Prof. Sinesio Pesco

Rio de Janeiro
September 2016



Yulieth Alzate Cardona

Object-based Modeling of Turbidite Lobes using Single-valued B-Splines

Dissertation presented to the Programa de Pós-graduação em Matemática of the Departamento de Matemática do Centro Técnico Científico da PUC-Rio, as partial fulfillment of the requirements for the degree of Mestre.

Prof. Sinesio Pesco

Advisor

Departamento de Matemática - PUC-Rio

Prof. Abelardo Borges Barreto Junior

Departamento de Engenharia Mecânica - PUC-Rio

Prof. Helio Côrtes Vieira Lopes

Departamento de Informática - PUC-Rio

Prof. Lis Ingrid Roque Lopes Custódio

Instituto Politécnico do Rio de Janeiro - UERJ

Prof. Márcio da Silveira Carvalho

Coordinator of the Centro Técnico Científico da PUC-Rio

Rio de Janeiro, September 16th, 2016

All Rights Reserved.

Yulieth Alzate Cardona

Has a degree in Mathematics from Universidad Nacional de Colombia, Colombia.

Bibliographic card

Alzate Cardona, Yulieth

Object-based Modeling of Turbidite Lobes using Single-valued B-Splines / Yulieth Alzate Cardona; advisor: Sinesio Pesco. — 2016.

69 f: il. ; 30 cm

Dissertação (mestrado) - Pontifícia Universidade Católica do Rio de Janeiro, Departamento de Matemática, 2016.

Inclui bibliografia.

1. Matemática – Dissertação 2. Lobos Turbidíticos; 3. Modelagem Baseada em Objetos; 4. B-Splines univalorados. I. Pesco, Sinesio. II. Pontifícia Universidade Católica do Rio de Janeiro. Departamento de Matemática. III. Título.

CDD: 510

A mi esposo por su amor, su fe y su apoyo constante...
Gracias.

Acknowledgement

I would first like to thank the CNPq and PETROBRAS for the financial support and the bibliographic contributions that allowed the development of this project.

I wish to express my sincere gratitude to Professor Sinesio Pesco for sharing his knowledge and introduce me a whole new area for me, also for his infinite patience and his wonderful guidance conducting this work.

Besides my advisor, I would like to thank the reviewers for the time spent reading this work and their suggestions to improve it.

I also thank to Creuza, who always takes care of all students, to all administrative and academic staff of the Mathematics Department for their help and kindness.

I must express my very profound gratitude to all my family in particular my parents, my sisters and to my nephew for providing me support and continuous encouragement throughout my years of study. I would also like to thank my friends who supported me, and incited me to strive towards my goal. This accomplishment would not have been possible without them. Thank you.

Lastly, I owe thanks to a very special person, my husband, Heber for his continued and unfailing love, support and understanding during my pursuit of Master degree that made the completion of the dissertation possible.

Abstract

Alzate Cardona, Yulieth; Pesco, Sinesio (Advisor). **Object-based Modeling of Turbidite Lobes using Single-valued B-Splines.** Rio de Janeiro, 2016. 69p. MSc. Dissertation — Departamento de Matemática, Pontifícia Universidade Católica do Rio de Janeiro.

Turbidity currents are gravitational flows that have higher density than its surroundings, and they are characterized by having a turbulent appearance and by moving at high speed carrying out a transfer process sediment. The problem addressed in this thesis is the modelling of turbidities deposits. It will be taken based on a depositional model that contains three turbidities lobes. Our contribution is to develop a object-based model using Single-valued B-Spline to simulate turbidities reservoirs in a regular Cartesian grid.

Keywords

Turbidities Lobes; Object-Based Modelling; Single-valued B-spline.

Resumo

Alzate Cardona, Yulieth; Pesco, Sinesio. **Modelagem baseada em objetos de Lobos Turbidíticos usando B-Splines univalorados.** Rio de Janeiro, 2016. 69p. Dissertação de Mestrado — Departamento de Matemática, Pontifícia Universidade Católica do Rio de Janeiro.

As correntes de turbidez são fluxos gravitacionais que têm uma densidade mais elevada do que o seu entorno, sendo caracterizadas por terem uma aparência turbulenta e por moverem-se com uma alta velocidade, realizando um processo de transferência de sedimentos. O problema abordado nesta tese é a modelagem de depósitos turbidíticos baseada em um modelo deposicional com três lobos turbidíticos. A principal contribuição foi desenvolver um modelo baseado em objectos usando B-Splines univalorados para simular reservatórios de turbiditos em um grade cartesiana regular.

Palavras-chave

Lobos Turbidíticos; Modelagem Baseada em Objetos; B-Splines univalorados.

Contents

1	Introduction	12
1.1	Motivation	12
1.2	Objective	12
1.3	Methodology	14
1.4	Description	14
2	Preliminaries	16
2.1	Mathematical concepts for modelling	16
2.2	Turbidities	22
3	Modelling	24
3.1	Conceptual model	24
3.2	Modeling of the geological body	25
4	Results	42
4.1	Establishing the basic parameters	42
4.2	Simulation of turbidity	43
5	Conclusion	62
5.1	Conclusions of the project	62
5.2	Future works	63
	Bibliography	65
	Appendix A	67

List of figures

1.1	Depositional model.	13
1.2	Geometric model.	14
2.1	Bézier curves.	17
2.2	The Bernstein polynomials for $n = 4$.	18
2.3	Control points.	18
2.4	The recursive definition of <i>B-Spline basis functions</i> (Piegl and Tiller, 1996).	19
2.5	Polygon and control points of a <i>B-Spline curve</i> .	20
2.6	Example of Single-valued B-Spline curves.	21
2.7	Turbidity deposit (Pessini, 2013).	23
3.1	Main parameters of turbidities.	25
3.2	Examples of grids.	26
3.3	Grid structure.	26
3.4	Part of the grid filled with 1's to contain information about the object.	27
3.5	Example of model differentiating two parts of a figure, top and bottom.	28
3.6	Grid filled according to the respective part of the object.	28
3.7	Grid filled.	29
3.8	Parameters.	29
3.9	Width and thickness parameters.	30
3.10	Body geometry.	30
3.11	Turbidities lobes.	31
3.12	B-Spline curves.	32
3.13	Control points t_{sup} .	33
3.14	Control points w_{right} .	34
3.15	B-Spline curve to t_{sup} .	34
3.16	B-Spline curve to w_{right} .	35
3.17	B-Spline curves of turbidities lobes.	36
3.18	B-Spline curves contour.	36
3.19	Connecting the B-Spline curves.	37
3.20	Transversal contour of the turbidity.	37
3.21	Transversal contour of the turbidity.	38
3.22	Limiting the grid.	39
3.23	Center of the grid.	40
4.1	Domain and dimensions of the grid.	42
4.2	Simulation resulting turbidity, example 1.	44
4.3	Simulation resulting turbidity, example 2.	46
4.4	Simulation resulting turbidity, example 3.	47
4.5	Simulation resulting turbidity, example 4.	49
4.6	Simulation resulting turbidity, example 5.	50
4.7	Simulation resulting turbidity, example 6.	52

4.8	Simulation resulting turbidity, example 1.	54
4.9	Simulation resulting turbidity, example 2.	55
4.10	Simulation resulting turbidity, example 3.	57
4.11	Simulation resulting turbidity, example 4.	58
4.12	Simulation resulting turbidity, example 5.	60
4.13	Simulation resulting turbidity, example 6.	61
5.1	Simulation of channels with the same origin and bounded length.	64
5.2	Parameter file.	69

List of tables

4.1	Parameters of turbidity.	43
4.2	Parameters of turbidity example 1.	45
4.3	Parameters of turbidity example 2.	45
4.4	Parameters of turbidity example 3.	48
4.5	Parameters of turbidity example 4.	48
4.6	Parameters of turbidity example 5.	51
4.7	Parameters of turbidity example 6.	51
4.8	Parameters of turbidity example 1.	53
4.9	Parameters of turbidity example 2.	56
4.10	Parameters of turbidity example 3.	56
4.11	Parameters of turbidity example 4.	59
4.12	Parameters of turbidity example 5.	59
4.13	Parameters of turbidity example 6.	61

1 Introduction

1.1 Motivation

Turbidity currents are gravitational flows that are usually caused by natural catastrophic events of different types, such as a storm surges, shocks induced by earthquakes, failure of sediments on slopes, river floods, etc. Turbidity currents move as a flow of high-speed and higher density in deep waters of the sea or a lake, making it difficult to study.

These currents generate deposits with a denser base and an upper portion with a turbid appearance, this is the reason for using the name “turbidity current”, at the same time that “turbidities” is used for representing the deposits resulting by turbidity currents.

The study of turbidities was motivated by military interest to anticipate and trace the routes of submarines; then an interest of an economic nature awoke as it began to observe some relation between turbidity deposits and oil reservoir. About 90% of Brazil’s oil reserves discovered by Petrobras, are contained in deposits generated by turbidity currents and/or similar gravitational flows; therefore the study and modelling of hydrocarbon reservoirs, particularly turbidity deposits, is of great importance in the oil field when exploring a reservoir (for more details see (Paim et al., 2003)).

1.2 Objective

As mentioned above, since the turbidities are hydrocarbon deposits related to oil reservoirs, they are a subject of great interest in research oil; therefore the main objective of this work is to estimate the geometry of these geological bodies to model a possible scenario that closely matches the actual

spatial distribution of these bodies.

Turbidity currents are important sediment transfer processes of shallow waters to deeper waters, such processes are characterized by forming depositional systems within an environment of deep water.

In this way, we use a depositional model that contains three turbidity lobes with different thickness; it is considered the first litter formed by a stream of initial turbidity and the third as the last level by a turbidity current generated.

The modelling of hydrocarbon reservoirs is very attractive in research projects oilfield, because it helps to have a better understanding of the distribution of deposits. Our interest is to generate a geometric design of these geological bodies with object-based modelling, using *B-Spline curves*. At the end we will have some simulations of possible scenarios of turbidities deposits with three lobes. The development of the algorithm is based on the search for a solution to the problem of simulation turbidities deposits. Given the limited information on these objects, we will develop a simplified model of the reservoir.

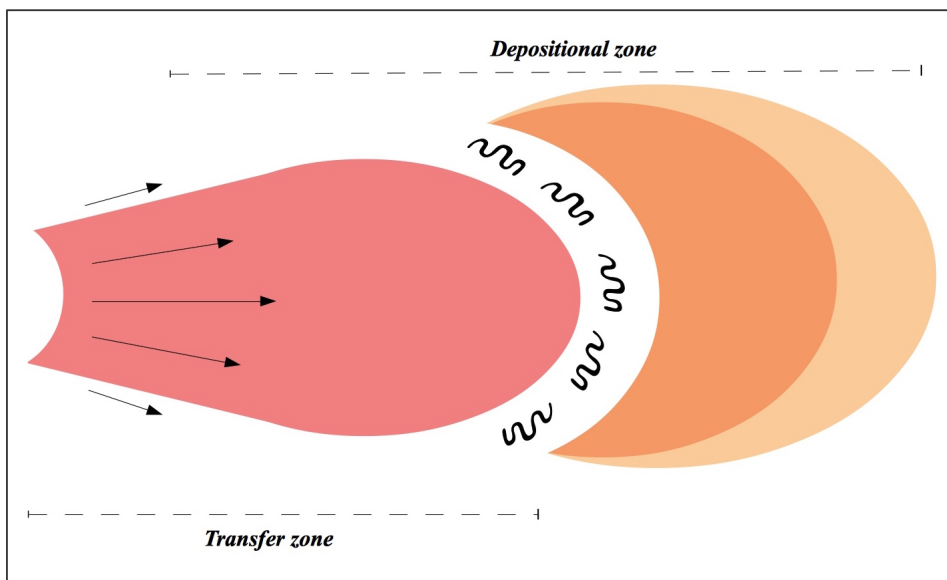


Figure 1.1: Depositional model.

1.3 Methodology

Turbidity currents generate turbidity reservoir; following a depositional model they will be defined different variables and parameters that fit the geometry of the body, so that through a simulation based on objects we can model a turbidity reservoir with three lobes which represent three layers generated by different turbidity current.

This type of reservoirs determine almost all oil produced in Brazil, so the study and creating a possible scenario through simulation based on objects could be a great tool in the development of oil research.

To carry out our simulation process, it was necessary to study the geometry of the model chose and properly define the parameters to depict independently different characteristics of the geological body. To represent the turbidity lobe, we use a Boundary representation model, B-Rep model for short (Mäntylä, 1988), defined by Single-valued B-Spline to model the directrix curve, using a similar process introduce by Sánchez-Reyes (Sánchez-Reyes, 1994) to modelling the surface.

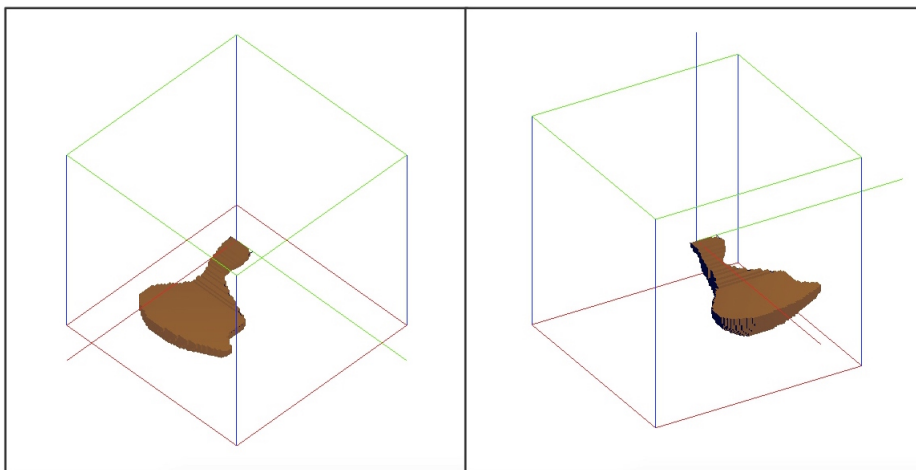


Figure 1.2: Geometric model.

1.4 Description

This thesis is divided into four parts. The first one contains the mathematical concepts required for the theoretical development work as well as some geological definitions that will serve the reader to enter into the modelling process of our geological body. It also shows us quickly a description of the

geological problem to be worked throughout this work.

The second part consists of a step by step explanation to the process carried out to obtain the desired simulations. It shows the construction of all objects used in modelling, the geometry chosen for the geologic body and the manner in which the contour is designed to obtain a satisfactory simulation. Furthermore, the way of generating output data representing the geological simulation body according to the selected characteristics is explained.

In the third part, we show the simulations obtained with the model chosen as different examples of possible difficulties of work. Finally, the last part is a summary of the objectives achieved and generated concerns that lead to future questions.

2 Preliminaries

In this chapter we present the required mathematical and geological concepts necessary in this work.

2.1 Mathematical concepts for modelling

This section describes the definitions of *Bézier curves* and *B-Spline curves parametric and Single-valued*. We also show some important properties of these curves and exhibit examples of the different *B-Spline curves*.

2.1.1 Bézier curves

In modelling is common to represent curves by means of *implicit equations* or *parametric functions*. A curve described by an implicit equation is a curve whose points of coordinates (x, y) satisfy an implicit relationship of the form $f(x, y) = 0$. A curve represented parametrically is one where each coordinate is presented as an explicit function of an independent parameter

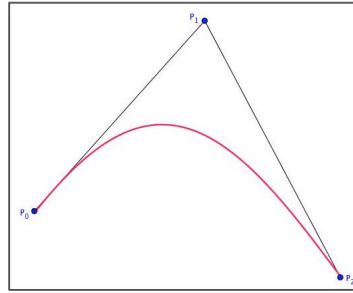
$$\mathbf{C}(u) = (x(u), y(u)), \quad a \leq u \leq b.$$

The Bézier curves are parametric polynomial curves, expressed in terms of Bernstein polynomials for their coordinate functions (Farin, 2002).

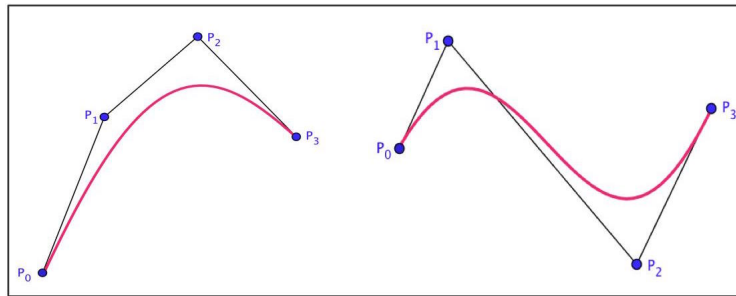
Definition 2.1. *An n th-degree Bézier curve is defined by*

$$\mathbf{C}(u) = \sum_{i=0}^n B_{i,n}(u) \mathbf{P}_i, \quad 0 \leq u \leq 1.$$

*The basis functions, $B_{i,n}(u)$, are the classical n th-degree Bernstein polynomials and the geometric coefficients \mathbf{P}_i are called **control points**.*



2.1(a): Quadratic.



2.1(b): Cubic.

Figure 2.1: Bézier curves.

Definition 2.2. The *Bernstein polynomials* are defined explicitly by

$$B_{i,n}(u) = \binom{n}{i} u^i (1-u)^{n-i},$$

where the binomial coefficients are given by

$$\binom{n}{i} = \begin{cases} \frac{n!}{i!(n-i)!} & \text{if } 0 \leq i \leq n \\ 0 & \text{else.} \end{cases}$$

Some properties of Bernstein polynomials are:

- They are linearly independent.
- They are symmetric, that is

$$B_{i,n}(u) = B_{n-i,n}(1-u).$$

- The only roots are 0 and 1, more precisely,

$$B_{i,n}(0) = B_{n-i,n}(1) = \begin{cases} 1 & \text{for } i = 0 \\ 0 & \text{for } i > 0 \end{cases}.$$

- Partition of unity,

$$\sum_{i=0}^n B_{i,n}(u) = 1, \quad \forall u \in \mathbb{R}.$$

- They are positive in $(0, 1)$:

$$B_{i,n}(u) > 0, \quad \text{for } u \in (0, 1).$$

- Satisfy the recurrence relation

$$B_{i,n+1}(u) = uB_{i-1,n}(u) + (1-u)B_{i,n}(u),$$

where $B_{-1,n} \equiv B_{n+1,n} \equiv 0$ and $B_{0,0} \equiv 1$.

The figure (2.2) is an example of Bernstein polynomials of 4-degree. For a four degree there are five polynomials over the interval.

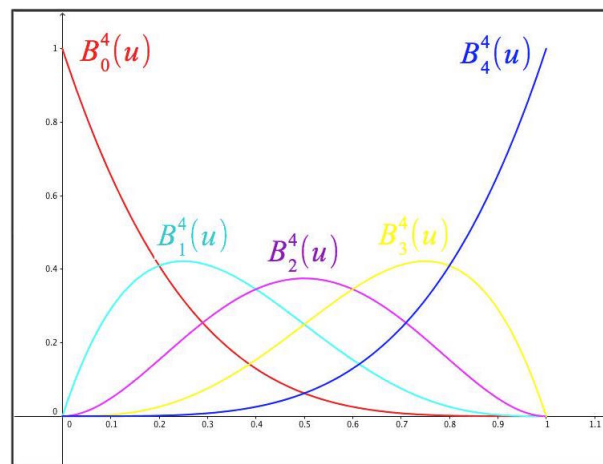


Figure 2.2: The Bernstein polynomials for $n = 4$.

The *control points* are essential elements in a *Bézier curve*, as they are responsible for defining the shape of the curve (see figure 2.3), that is, by moving the control points the curve changes its design.

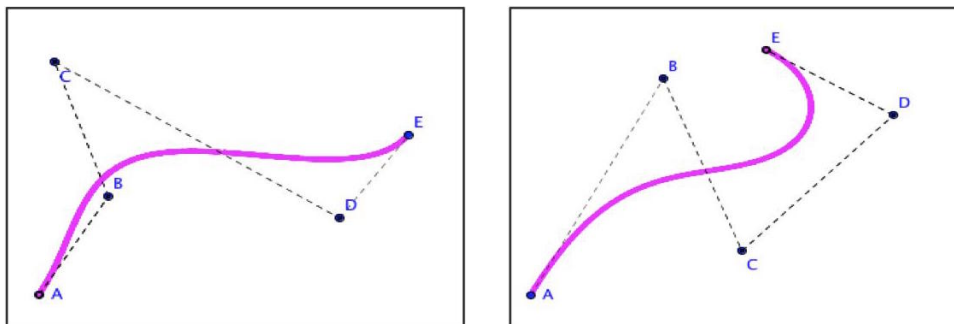


Figure 2.3: Control points.

2.1.2 B-Spline curves

B-Splines curves consist of many polynomial pieces, offering much more versatility than the *Bézier curves*. Many *B-Splines curves* properties can be understood by considering just one polynomial piece (Piegl and Tiller, 1996).

Definition 2.3. Let $U = \{u_0, \dots, u_m\}$ be a non-decreasing sequence of real numbers, i.e., $u_i \leq u_{i+1}$, $i = 0, \dots, m - 1$. The u_i are called **knots**, and U is the **knot vector**. The i -th **B-Spline basis function** of p -degree (order $p+1$), denoted by $N_{i,p}(u)$, is defined as

$$N_{i,0}(u) = \begin{cases} 1 & \text{if } u_i \leq u \leq u_{i+1} \\ 0 & \text{otherwise} \end{cases} \quad (2.1)$$

$$N_{i,p}(u) = \frac{u - u_i}{u_{i+p} - u_i} N_{i,p-1}(u) + \frac{u_{i+p+1} - u}{u_{i+p+1} - u_{i+1}} N_{i+1,p-1}(u).$$

Note that

- $N_{i,0}(u)$ is a step function, equal to zero everywhere except on the half-open interval $u \in [u_i, u_{i+1})$;
- for $p > 0$, $N_{i,p}(u)$ is a linear combination of two $(p - 1)$ -degree basis (figure 2.4);

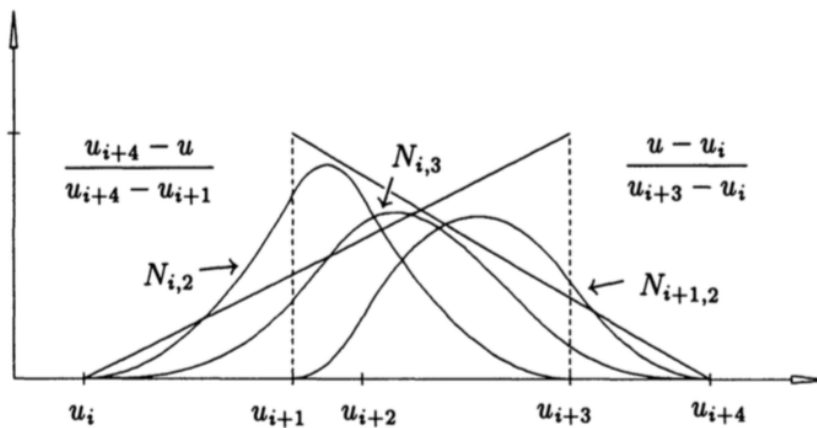


Figure 2.4: The recursive definition of *B-Spline basis functions* (Piegl and Tiller, 1996).

- computation of a set of basis functions requires specification of a knot vector, U , and the degree, p ;
- the equation (2.1) can yield the quotient $0/0$; we define this quotient to be zero;
- the $N_{i,p}(u)$ are piecewise polynomials, defined on the entire real line; generally only the interval $[u_0, u_m]$ is of interest;

- the half-open interval, $[u_i, u_{i+1})$, is called the *ith knot span*; it can have zero length, since knots need not be distinct.

Definition 2.4. A *p*th-degree **B-spline curve** is defined by

$$\mathbf{C}(u) = \sum_{i=0}^n N_{i,p}(u) \mathbf{P}_i \quad a \leq u \leq b, \quad (2.2)$$

where the $\{\mathbf{P}_i\}$ are the control points, and the $\{N_{i,p}(u)\}$ are the *p*th-degree B-Spline basis functions (equation 2.1) defined on the non-periodic (and non-uniform) knot vector

$$U = \{\underbrace{a, \dots, a}_{p+1}, u_{p+1}, \dots, u_{m-p-1}, \underbrace{b, \dots, b}_{p+1}\}$$

($m + 1$ knots). Unless stated otherwise, we assume that $a = 0$ and $b = 1$. The polygon formed by the $\{\mathbf{P}_i\}$ is called the control polygon.

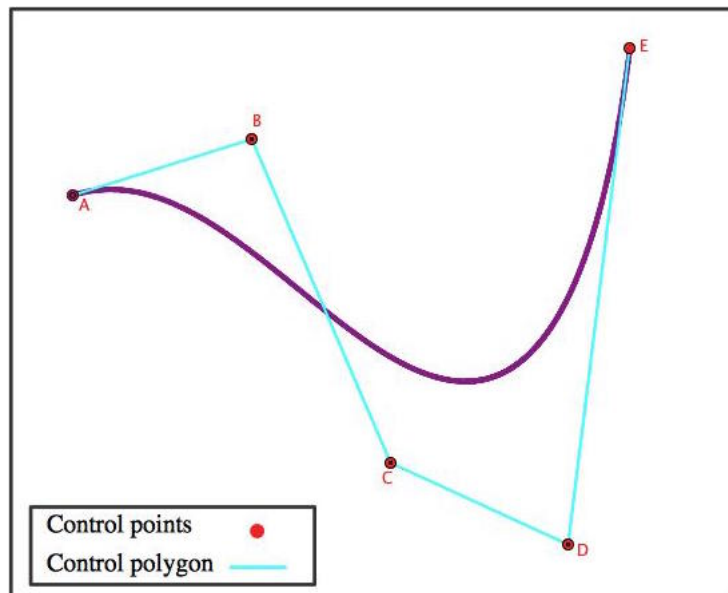


Figure 2.5: Polygon and control points of a *B-Spline curve*.

2.1.3 Single-valued curves

Single-valued B-Spline curves are a type of planar B-Spline curves non-rational used to approximate the curve $y = f(x)$ in Cartesian coordinates (x, y) (Sánchez-Reyes, 1994), where f denotes a polynomial (or $z = g(x)$ in the plane (x, z) with g a polynomial).

A curve $\mathbf{C}(u)$ of degree m is defined by a sequence of nodes $\{u_0, \dots, u_{n+2(m-1)}\}$, such that, its domain is restricted to $u \in [u_{m-1}, \dots, u_{n+(m-1)}]$

and the curve is defined in n intervals. Since the curve is Single-valued, their control points are $P_i = (x_i, y_i)$ where

$$x_i = \frac{1}{n}[u_i + \dots + u_{i+(m-1)}], \quad i = 0, \dots, n + (m - 1). \quad (2.3)$$

These planar curves can be written in the form:

$$\mathbf{C}(u) = \begin{bmatrix} x(u) \\ y(u) \end{bmatrix} = \begin{bmatrix} u \\ f(u) \end{bmatrix}.$$

We are interested in functions f that are expressed in terms of the B-Spline basis functions:

$$f(u) = \sum_{i=0}^{n+(m-1)} y_i N_{i,m}(u).$$

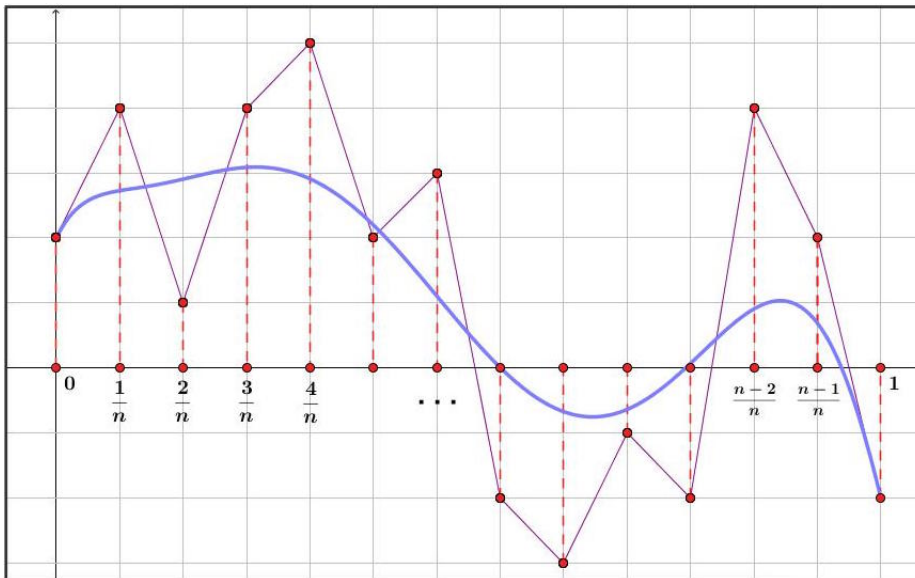


Figure 2.6: Example of Single-valued B-Spline curves.

In our work we will use Single-valued B-Spline curves to define the directrix curve of the lobe object. This kind of curve will be important to make easy the *in_out* test in the grid; in chapter three will be explained in more detail the importance of choosing simple nodes spaced evenly over in an interval to determine the control points of the B-Spline curve.

2.2 Turbidities

Our main object of study is the turbidities deposits geological bodies; to have a better context, we will study some basic geological concepts that will help us get into the main objective of this work.

We will use the following concepts to describe our geological body to be studied (for a more detail study of turbidities see (Pessini, 2013)).

Definition 2.5. *The **turbidities** are defined as deposits resulting from turbidity currents, a type of gravitational flow, compound by layers.*

For our purposes, we will consider the turbidities regardless of the environment in which they are formed.

Quoting Pessini (Pessini, 2013), the turbidities deposits are characterized by a complex of sand bodies distributed channels and lobes, in very deep water. Also they are characterized by depositional settings. The fundamental expression of these systems is huge accumulations of basinal, cyclically-stacked sandstone lobes with an lateral extent. These accumulations, representing potential reservoirs, record the main depositional zone of large-volume turbidity currents originated from hyperpicnal flows (Bischoff et al., 2007).

The turbidity currents spread out to form a lobe of turbidities deposits that occupy a portion of the fan surface. An individual lobe is constructed by a succession of turbidity currents that tend to deposit further and further out on the lobe through time.

Following the already mentioned model, we study the turbidities deposits with three depositional lobes (figure 2.7).

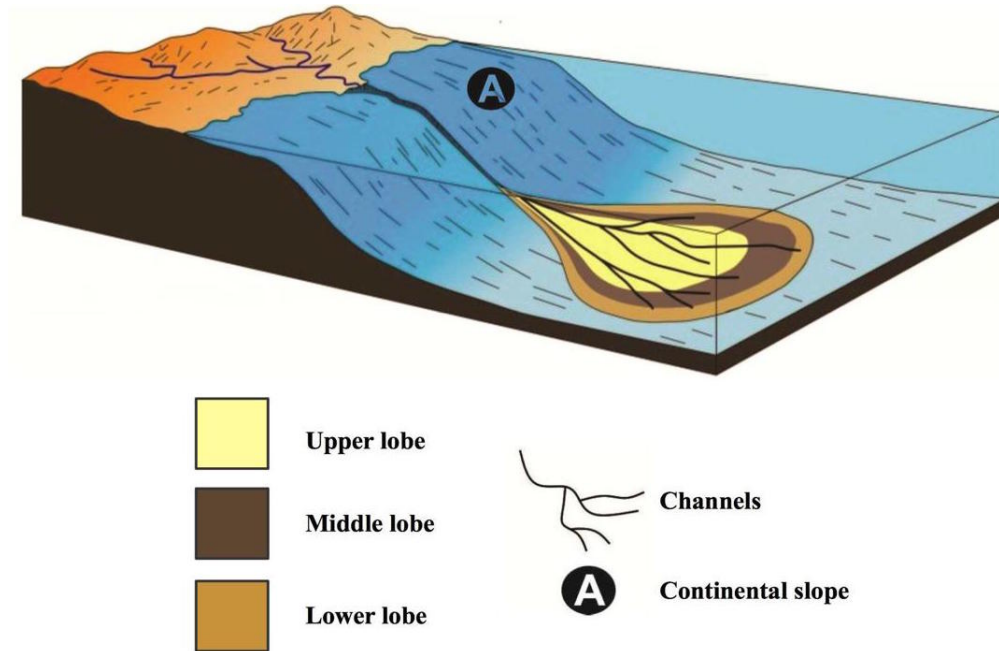


Figure 2.7: Turbidity deposit (Pessini, 2013).

3 Modelling

In this work we are interested in making more realistic models or representations of a space object being studied, which will be unconditioned.

This chapter explains the process that our computational modelling work follows. The first section illustrates the construction of the computational tools that will be used in order to model the geological body, and in the second section these tools will be connected with the mathematical concepts studied in chapter two, thus obtaining a prototype that can be interpreted in a successful way. The method by which they are interpreted or classified the resulting data will be shown in section three.

3.1 Conceptual model

Object-based simulation is an essential tool for building models using previously known methods. This work presents an option for object-based modelling turbidities lobes. The features of this model include a simple approach to place turbidities lobes within a depositional system; modelling techniques based on objects are widely applicable to modelling simple systems turbidities deposits with three lobes.

The figure 3.1 illustrates our conceptual geometric model for modelling of turbidities deposits adopted in this work. There are three levels of lobes, we simulate following geometric specifications of each and generate their forms accordance with the model chosen. The first lobe is the deepest, which is considered the largest; once established the parameters for the first, the second and third lobe will be simulated in depositional way, depending on the features.

As shown in the figure 3.1, the model chosen has a simple geometry to be modelled using different parameters considering the shape of the body, i.e. considering length, width and thickness.

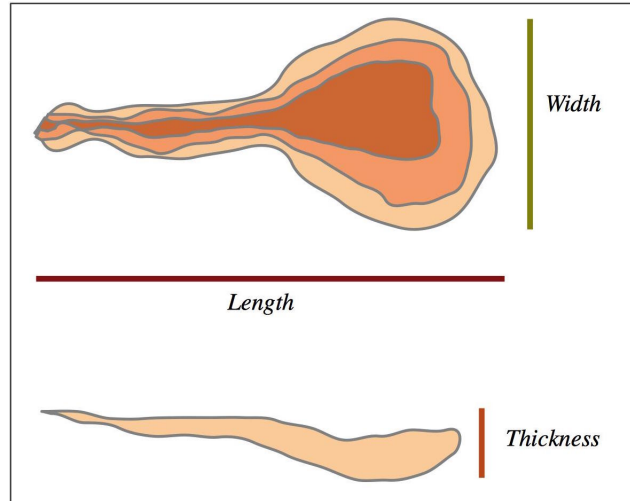


Figure 3.1: Main parameters of turbidities.

The result of the object-based simulation will be placed in a regular grid, which will be the input of a flow simulator. So in the next section we describe how the regular grid has been defined and then we describe the modelling of turbidity lobes.

3.2

Modeling of the geological body

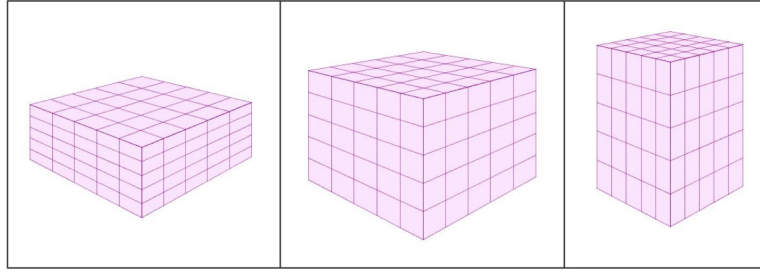
3.2.1

Grid object

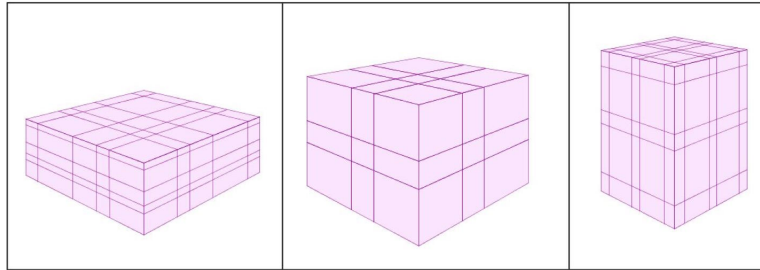
Definition 3.1. A *grid* in \mathbb{R}^3 is a tessellation of the space by parallelepipeds; these may be or not congruent. When parallelepipeds are congruent we say that is a **regular grid** and otherwise it will be called **irregular grid**. When we have a regular grid whose parallelepipeds are unit cubes, we will call it **Cartesian grid** (see definition in (Sanabria, 2016)).

In figure 3.2 we can see different examples of regular and irregular grids.

To start our process of building the model first we define our regular grid. The position of each rectangular parallelepiped is stored in a three dimensional matrix such that each input later can be used to identify and classify simulation data. This grid can be used to simulate a deposit which contains a geological body, in our case, a reservoir containing a turbidity will be simulated.



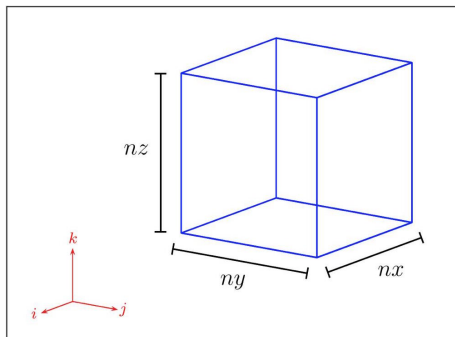
3.2(a): Regular grids.



3.2(b): Irregular grids.

Figure 3.2: Examples of grids.

In figure 3.3 we see the structure chosen for our Cartesian grid of \mathbb{R}^3 , with this type of grid we will work throughout the modelling process.



3.3(a): Dimensions of the grid.

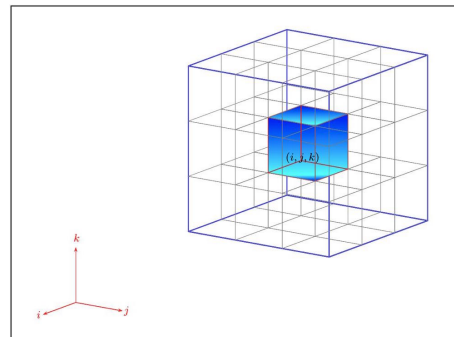
3.3(b): Cell (i, j, k) on the grid.

Figure 3.3: Grid structure.

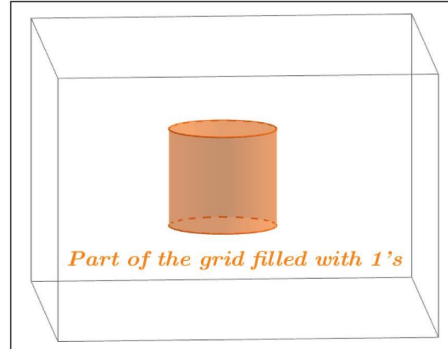
In the next step we define which cells of the grid will be marked. For this, define $g[i][j][k]$ as the corresponding *cell* at the position (i, j, k) of the grid, and consider $g[i][j][k]$ a way to represent a binary system that tells us if the cell either contains or does not contain the object of interest:

$$g[i][j][k] = \begin{cases} 1, & \text{if contains information about the object} \\ 0, & \text{otherwise.} \end{cases}$$

In figure 3.4 we have a grid filled with 1's and 0's identifying regions containing or not information about the object.

0	0	0	0	0	0	0	0
0	0	0	0	0	0	0	0
0	0	1	1	1	0	0	0
0	0	1	1	1	0	0	0
0	0	1	1	1	0	0	0
0	0	1	1	1	0	0	0
0	0	1	1	1	0	0	0
0	0	0	0	0	0	0	0

3.4(a): Grid filled.



3.4(b): Figure obtained.

Figure 3.4: Part of the grid filled with 1's to contain information about the object.

For the turbidities lobes simulation we need to modify the structure, because it will be not enough to fill 0's and 1's. In our modelling will be essential to distinguish which part of the object corresponding each cell marked with 1, for example if the purpose is to differentiate the top and bottom of the object. In this case:

- Initially, the grid will be filled with 1's in all cells; that is, $g[i][j][k] = 1$ for all values of i, j, k .
- We use a prime number to distinguished different layers:

$$PartA \rightarrow Number \ 2,$$

$$PartB \rightarrow Number \ 3.$$

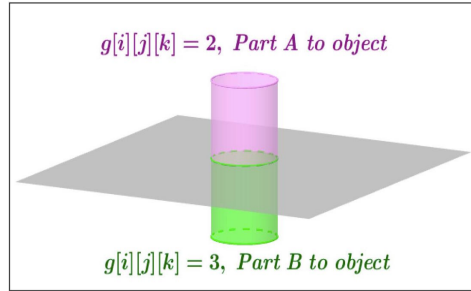
And so on, depending on how many parts have the object.

- In this way the cells containing information about the object will be redefined as follows (see figure 3.5):

$$g[i][j][k] = \begin{cases} 2 * g[i][j][k], & \text{if corresponds to Part A of the object} \\ 3 * g[i][j][k], & \text{if corresponds to Part B of the object.} \end{cases}$$

1	1	1	1	1	1	1	1	1
1	1	1	1	1	1	1	1	1
1	1	1	2	2	1	1	1	1
1	1	1	2	2	1	1	1	1
1	1	1	2	2	1	1	1	1
1	1	1	3	3	1	1	1	1
1	1	1	3	3	1	1	1	1
1	1	1	1	1	1	1	1	1

3.5(a): Grid filled.



3.5(b): Figure obtained.

Figure 3.5: Example of model differentiating two parts of a figure, top and bottom.

With this new way to identify the cells in the grid, the ability to distinguish more than one piece of the object to be modelled is acquired; which later will be very useful for simulating the three layers of turbidities lobes.

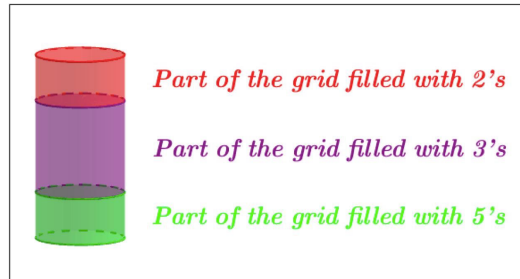
3.2.2 Turbidity parameters

An important part of any object-based modelling is the geometric shape and in this case we are considering a turbidity reservoir in a depositional model. Each object is a template of cells that would be coded according to the scheme in section 3.2.1 as follows (see figure 3.6):

- Upper lobe (Code 2)
- Middle lobe (Code 3)
- Lower lobe (Code 5).

1	1	1	1	1	1	1	1	1
1	1	2	2	1	1	1	1	1
1	1	2	2	1	1	1	1	1
1	1	3	3	1	1	1	1	1
1	1	3	3	1	1	1	1	1
1	1	3	3	1	1	1	1	1
1	1	5	5	1	1	1	1	1
1	1	5	5	1	1	1	1	1

3.6(a): Grid filled.



3.6(b): Figure obtained.

Figure 3.6: Grid filled according to the respective part of the object.

In our system, it is essential to be able to distinguish which part of each cell belongs to the turbidity as well as to recognize those cells that belong to more than one lobe. This ability makes the model to be available for future requirements. In order to attain this skill, the cells that belong to several lobes will be filled with the product of the corresponding numbers to each of the lobes of which is part. This can be seen in Figure 3.7.

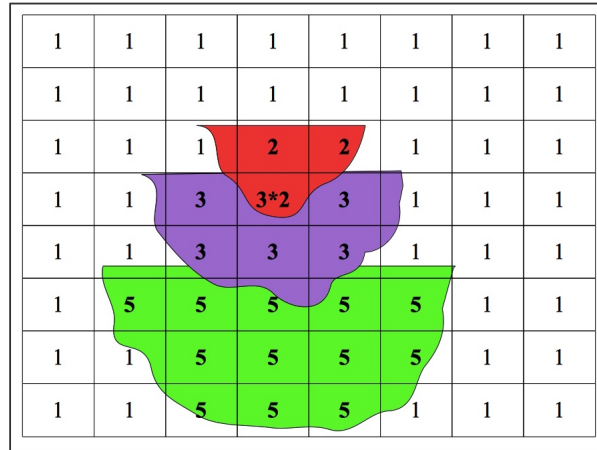


Figure 3.7: Grid filled.

The template provides advantages; however, the simulated realizations are sensitive to the choice of the size of the grid. The mesh size should be chosen large enough to preserve the geological formations represented by templates, but small enough to optimize the simulation time.

As can be seen in figure 3.8, the turbidities are defined by an *origin point* (x, y, z) , the *direction* \mathbf{d} , the *length* of the turbidity reservoir \mathbf{l} , *width* \mathbf{w} and *thickness* \mathbf{t} .

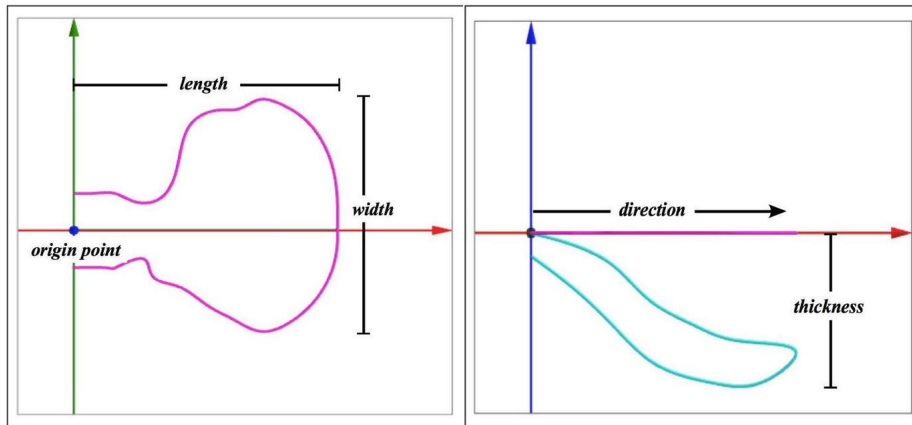


Figure 3.8: Parameters.

Both, the width and the thickness, will be defined by two independent parameters for each (see figure 3.9); that is, instead of considering only one width, two parameters are used to establish the maximum width to the central axis of turbidity (the axis that determines its direction): *width right* \mathbf{w}_r , and *width left* \mathbf{w}_l , independently; similarly two thickness or depths are defined, *thickness inf* \mathbf{t}_{inf} , and *thickness sup* \mathbf{t}_{sup} .

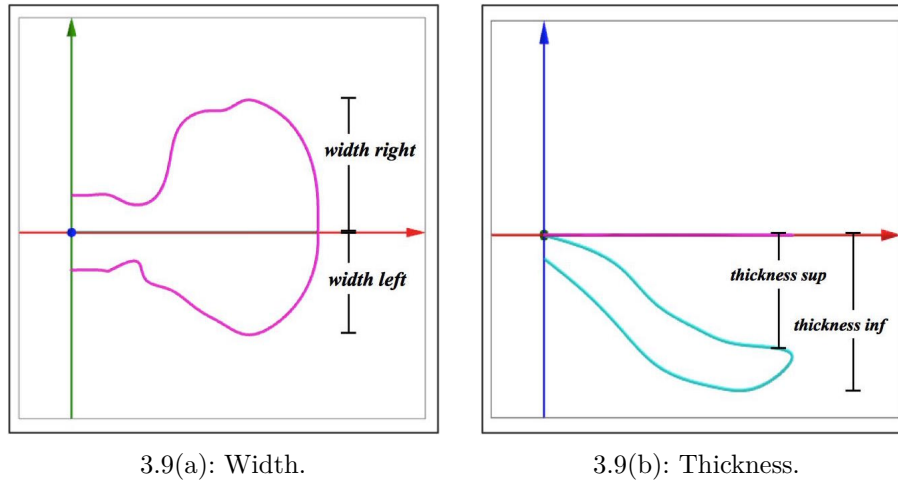


Figure 3.9: Width and thickness parameters.

Each parameter can take a range of possible values according to a probability distribution provided by the user. Keep in mind that turbidity width is measured perpendicular to the direction of the straight line of this and note that considering two separate widths have the freedom to shape deposits that are not necessarily symmetrical. Although, this work is limited in terms of spatial freedom of the parameters used, the approach has some advantages over object-based modelling on conventional turbidities. The input parameters used are geologically intuitive and accessible, in this way, we can control the size and the shape of the turbidities; besides the geometry of the simulated deposit can be made asymmetric, which makes the results more realistic.

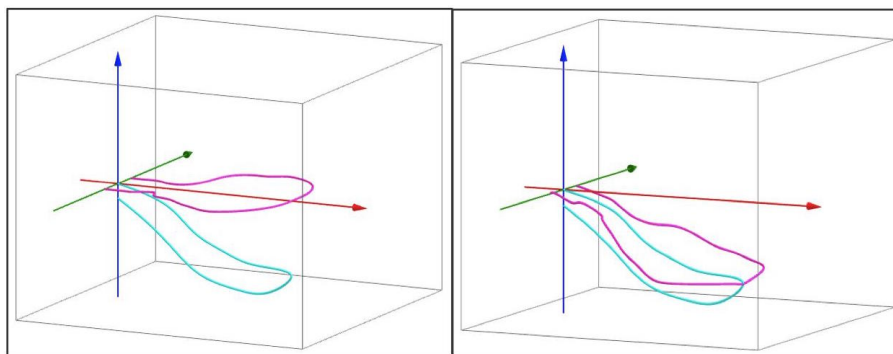


Figure 3.10: Body geometry.

The figure 3.10 shows the geometry adopted for a turbidity deposit. For simplicity, the geometric shape will remain fixed and only the size can vary.

The turbidity information is considered to define the parameters of the lobes; initially turbidity reservoir parameters are generated, which will become lower lobe parameters; taking these preliminary data, the variables for the

middle lobe and the upper lobe are generated. That is, the size of lobes depend on the size of turbidity; thus, a large turbidity generally has larger lobes (see figure 3.11).

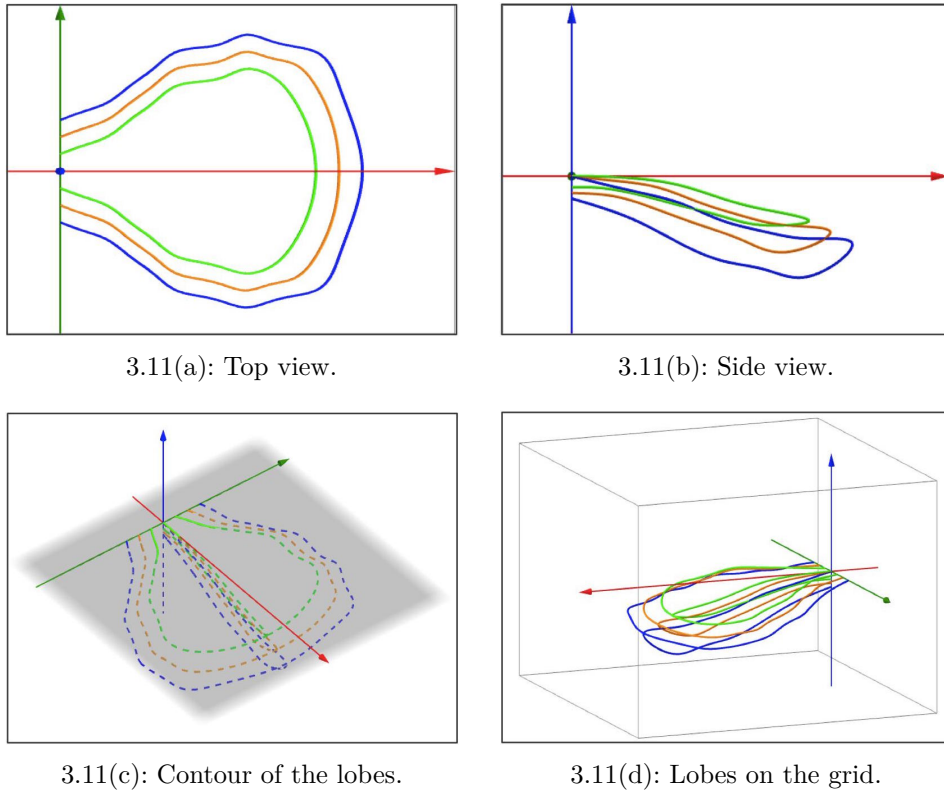


Figure 3.11: Turbidities lobes.

A complete list of the turbidity parameters is listed in the **Appendix A**.

The procedure to create a complete turbidity deposition from a defined model is simple:

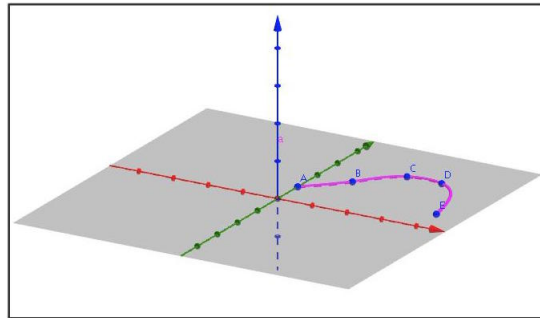
1. Initialize the grid as a three-dimensional matrix array, filling all entries with 1's.
2. Choose the corresponding values to different parameters that will be used to model the object.
3. Design the B-Spline curves which establish the geometry of the body and each of its components.
4. Assign to all cells within the turbidity deposit the required information for their classification of lower lobe / half lobe / upper lobe, as appropriate.

3.2.3 Modelling B-Spline curves

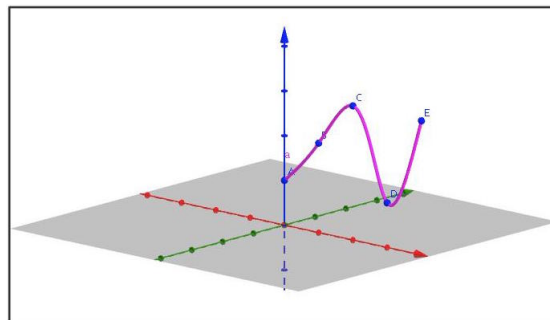
What follows is an sketch of the process performed for the final simulation. As mentioned above, the design of the *B-Spline curves* is very important for our purpose, because these curves defines the main directrix of the desired object. For the final object we must follow the steps: definition of the control points, design curves B-Spline, connect B-Spline curves and generate output data. In the following, we describe the first three steps and the last step will be present in the section 3.2.4.

Control points

The splines are simplified if the nodes are simple and are uniformly spaced; when nodes are equidistant, the B-spline is said to be uniform.



3.12(a): B-Spline on the xy plane.



3.12(b): B-Spline on the xz plane.

Figure 3.12: B-Spline curves.

In the design of the *B-Spline curves* we take a homogeneous partition of the interval over which the nodes are defined; in this case, the *abscissa*. The nodes will be the x coordinate of a set of points defined on an interval of the form $[0, a] \times 0 \times 0$; thus the control points of the *B-Spline curve* will lie on different Cartesian planes xy and xz (see figure 3.12).

By choosing nodes of the previously mentioned form, the control points will lose spatial freedom, since they will be conditional on x axis. The purpose of this “limitation” is to facilitate the classification of points in the grid when generating the in_out in the final simulation. When considering simple and homogeneous nodes the B -Spline curve is a function with respect to the variable x ; which can easily classify grid points depending on their location with respect to the graph of the function, that is, it may be decided whether a grid point is either right or left of the curve in the case of the xy plane and up or down in the case of the xz plane (see figure 3.12). This classification of the grid points is less expensive than if an implicit curve will be taken to decide whether points are inside or outside.

Control points are defined in terms of x and depend directly on the values given to the turbidities parameters.

We divided an interval $[0, a]$, on the abscissa axis, evenly into the number of points desired $n + 1$. Thus, we get the $n + 1$ points $\{0, a/n, \dots, a\} \in [0, a]$ which will be generated with the control points according to the parameters chosen.

Since each turbidity lobe has its own B-Spline curves, then each lobe will also have their own control points to generate each of its B-Spline curves. In the figures 3.13 and 3.14 we show a particular example to calculate the control points, giving some possible values of the parameters w_{right} and t_{sup} of a turbidity.

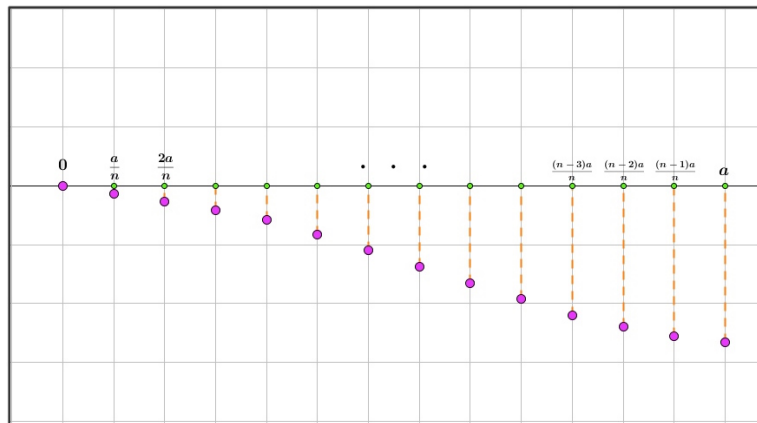


Figure 3.13: Control points t_{sup} .

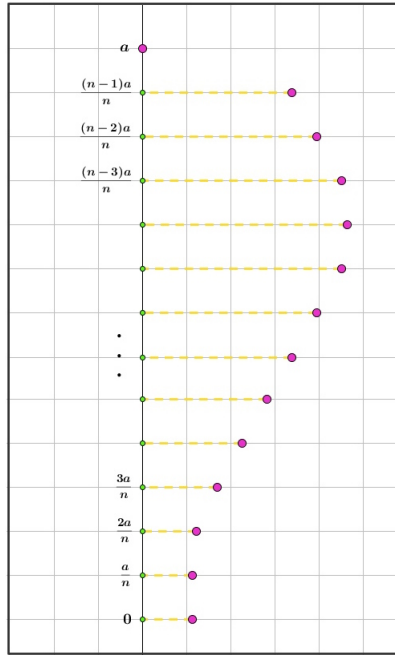


Figure 3.14: Control points w_{right} .

Design B-Spline curves

To design the B-Spline curves we have chosen fourteen control points for each of them; these control points are defined in terms of a homogeneous partition of an interval of the x axis, as shown above. Defining our control points in this way, we obtain a Single-valued B-Spline curve (see section 2.1.3); this B-Spline curve determines us the variables y and z as a function of the coordinate x . We define B-Spline curve with $p = 3$ (class C^2) and the control points have some degree of freedom given by the ability to change and choose the parameters of turbidity according to our specific needs.

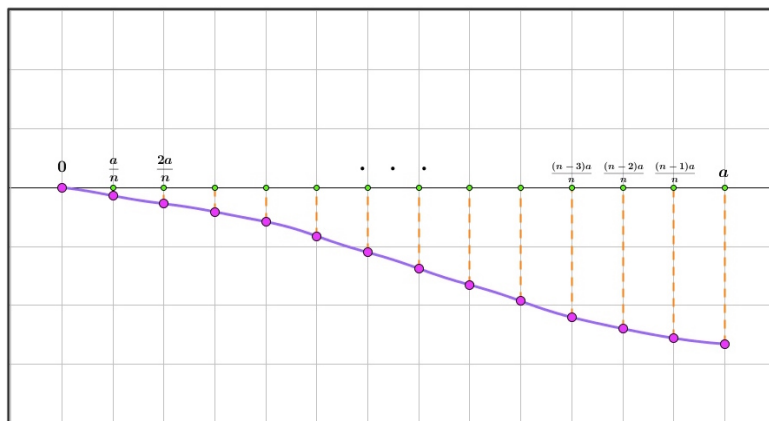
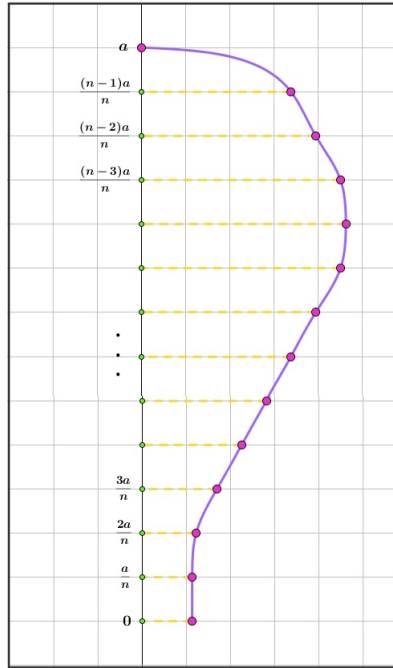


Figure 3.15: B-Spline curve to t_{sup} .

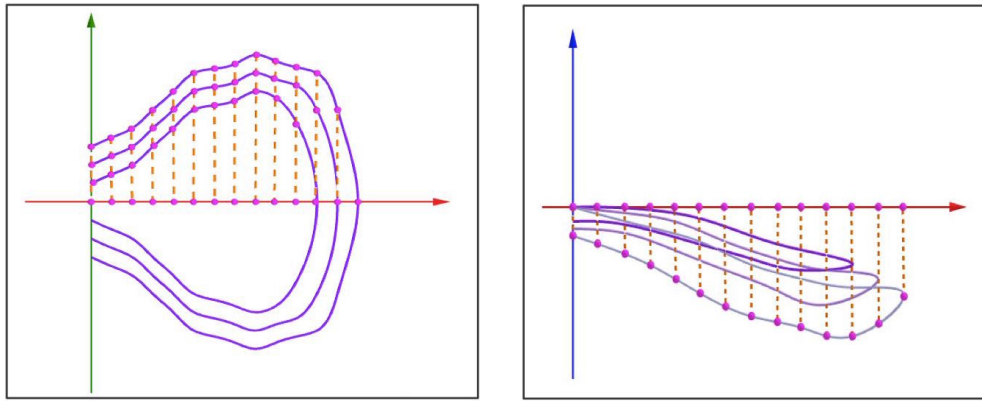
Figure 3.16: B-Spline curve to w_{right} .

We have used our conceptual model to define the lobe curves. First, we take the points on the axis to generate control points, with these points we build the top lobe using for B-Spline curves:

1. **First curve:** to fit the top of the lobe (t_{sup}) see figure 3.15.
2. **Second curve:** to fit the lower depth (t_{inf}) we build the next curve based on the curve constructed in the previous step, to ensure that this is below.
3. **Third curve:** to fit the right width (w_{right}) see figure 3.16.
4. **Forth curve:** to fit the left width (w_{left}) we build this curve analogously to right width.

After, we model the half lobe and the upper lobe using the same procedure. The depositional structure is made using a scalar parameter, we remove a checkpoint each time and reducing the initial value of the parameters used in the first lobe.

In figure 3.17 we can see the resulting B-Spline curves of each of the lobes.



3.17(a): B-Spline curves for width.

3.17(b): B-Spline curves for thickness.

Figure 3.17: B-Spline curves of turbidities lobes.

Connecting B-Spline curves

As mentioned above, the parameters that define the contour of turbidity are t_{sup} , t_{inf} , w_{right} and w_{left} , therefore to design each turbidity lobe, four curves B-Spline (one for each parameter) are necessary (see figure 3.18). After generating these curves, we must find an appropriate way to define the surface.

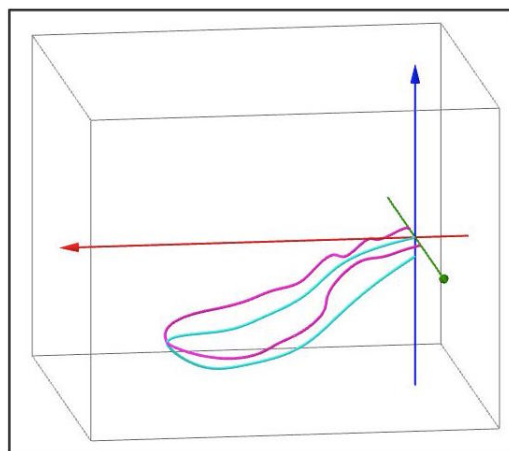


Figure 3.18: B-Spline curves contour.

For each two curves, we used a quarter of an ellipse as figure 3.19 shows. Since each lobe have four different B-Spline curves, then two quarter ellipses and two different straight segments will be needed to join the curves and to generate the turbidity deposit.

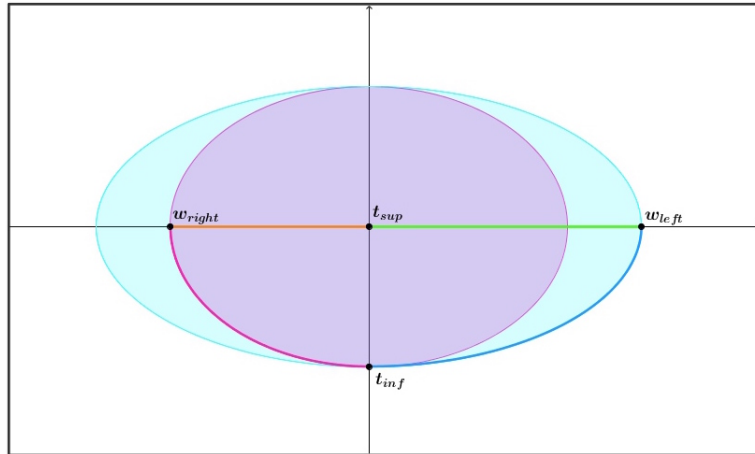


Figure 3.19: Connecting the B-Spline curves.

Each of the B-Spline curves corresponding to the width of the lobe (w_{right} and w_{left}) will be joined by a quarter ellipse with the B-Spline curve of the inferior thickness t_{inf} , and will be joined by a line segment with the B-Spline curve of the superior thickness t_{sup} . This can be seen in greater detail in figure 3.20.

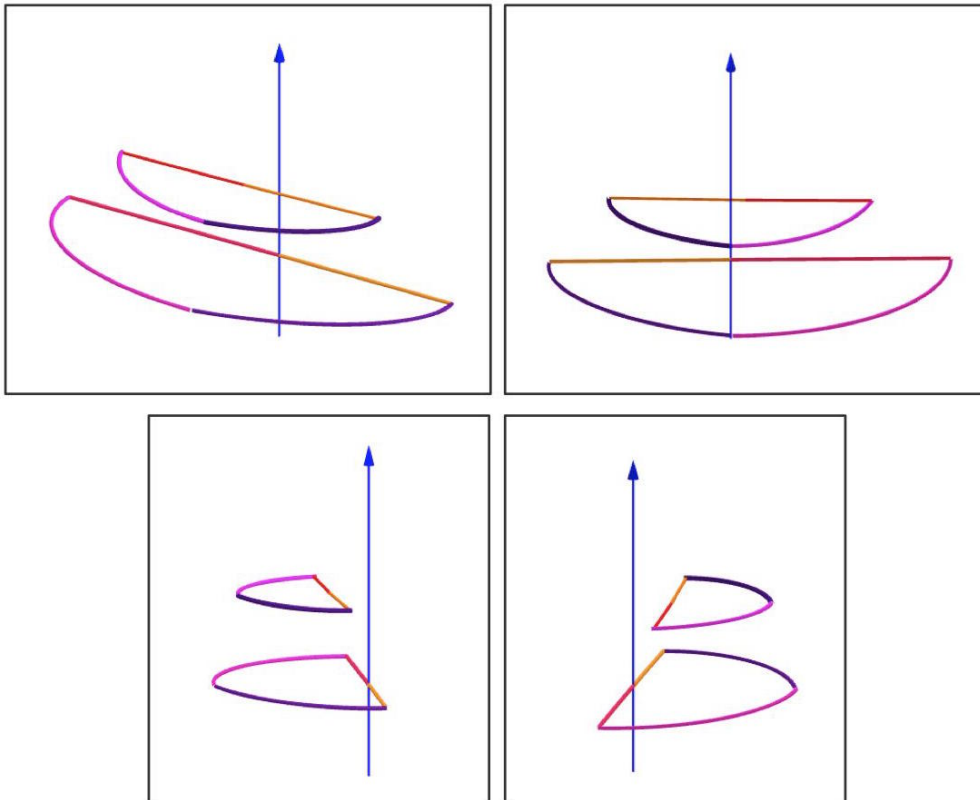


Figure 3.20: Transversal contour of the turbidity.

In figure 3.21 we can see more clearly that the contours of figure 3.20 are in different planes, both orthogonal to the x axis. This figure shows curves which limit the contour of two cross sections of a lobe turbidity from different angles of view.

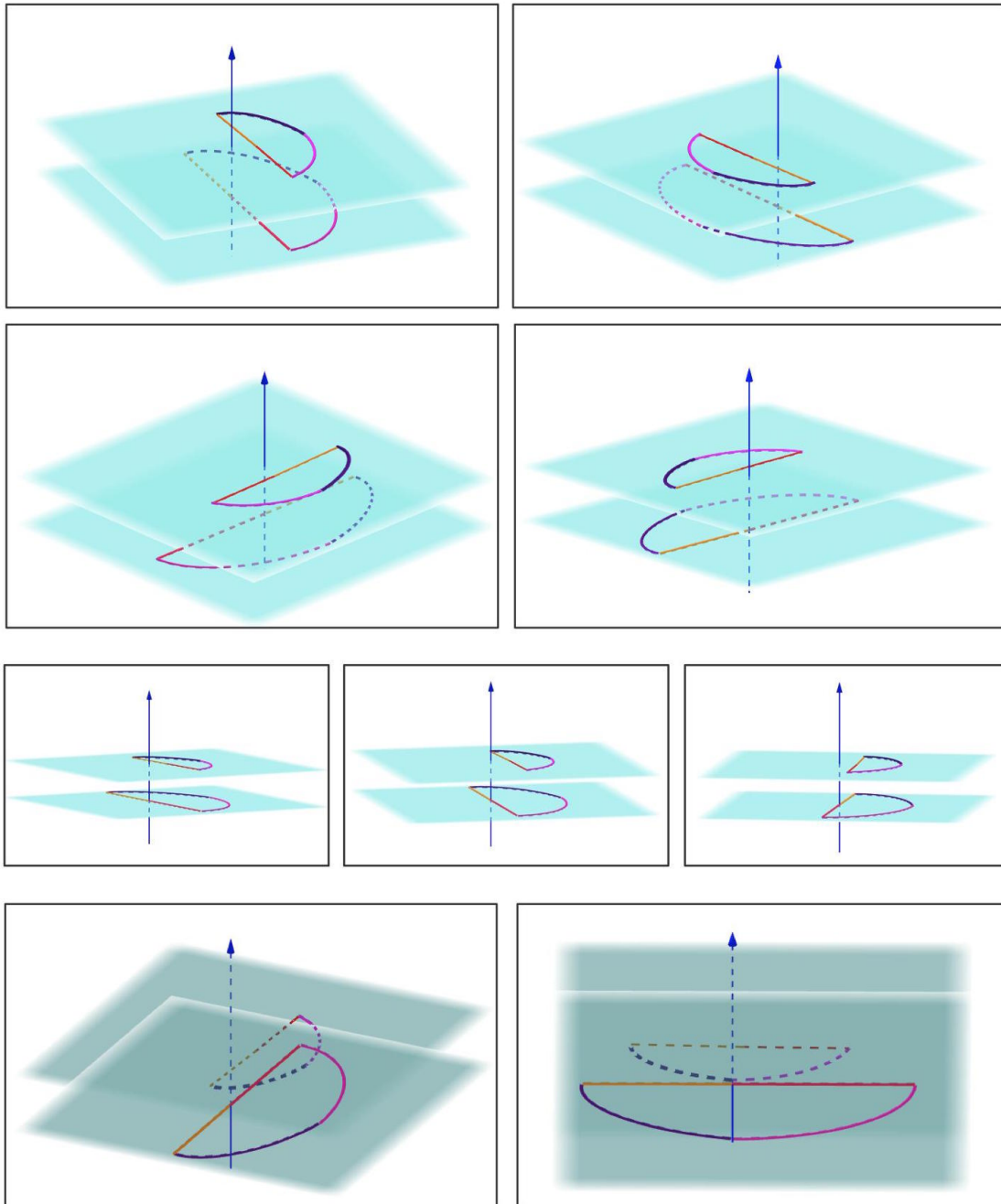


Figure 3.21: Transversal contour of the turbidity.

We can also see that these cross sections have the same widths and are at different thicknesses, these factors are determined by the parameters of each turbidity lobe; additionally, we would like to note that the width of the lateral ends with respect to the central axis is not the same, this is an advantage of

working with a width on the right and another on the left independently in the parameters w_{left} and w_{right} .

3.2.4 Output grid

When carrying out the simulation of the geological body, this can be located anywhere on the grid since its origin and direction are not fixed to the center of the grid, so when getting the final simulation will be necessary to test all points the grid and determine whether they are or not within the turbidity. In order to simplify the process, we moved the turbidity at the origin of the Cartesian axes, this is, the center of the grid to determine its overall length. By knowing this information it is possible to reduce the process tested around the grid to only a particular subregion by a parallelepiped contained within the initial grid (see figure 3.22).

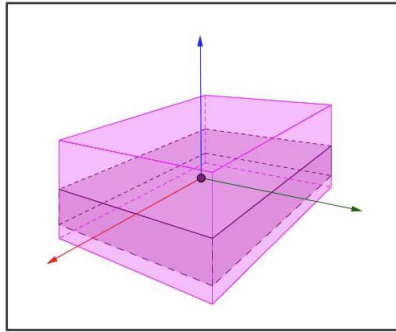


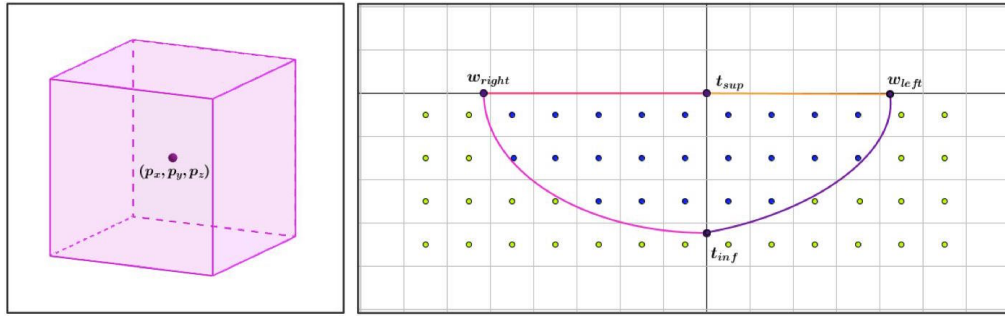
Figure 3.22: Limiting the grid.

Knowing the length required for said parallelepiped, this moves to the actual position of the turbidity; thus reducing the grid region to be tested.

The *in_out* test for the grid points should determine whether each grid cell is or not within the turbidity; for this, each cell will be represented for a point (p_x, p_y, p_z) indicating its center. Using the B-Spline curves, the quarter-ellipse and segments that limit the lobes, we can determine whether the cell belongs or not to the geological body. This is shown in figure 3.23.

To decide whether one point is inside the turbidity lobe, we create a function $g : \mathbb{R}^3 \rightarrow \{0, 1\}$ such that for a given point (p_x, p_y, p_z) :

$$g(p_x, p_y, p_z) = \begin{cases} 1, & \text{if } (p_x, p_y, p_z) \text{ is inside the turbidity} \\ 0, & \text{if } (p_x, p_y, p_z) \text{ is outside the turbidity.} \end{cases}$$



3.23(a): Center of the cell.

3.23(b): Testing the center of the cells.

Figure 3.23: Center of the grid.

This function g is responsible for selecting the points that will be considering inside the turbidity lobe. For each point (p_x, p_y, p_z) consider three steps:

1. **First component, p_x**

$$p_x \longrightarrow p_{x*} = p_x - x$$

2. **Second component, p_y**

$$p_y \longrightarrow p_{y*} = p_y - y$$

if $p_{y*} \geq 0$

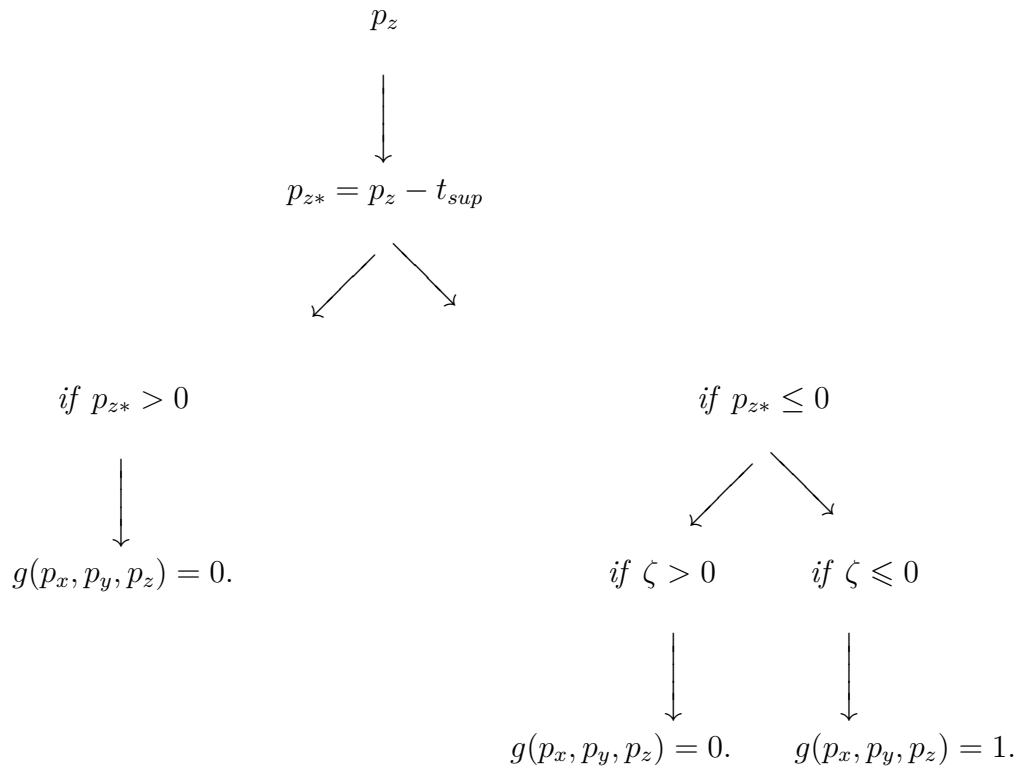
if $p_{y*} < 0$

$$\begin{aligned} &\downarrow \\ y_p &= w_{right}, \\ z_i &= t_{inf}, \\ z_s &= t_{sup}. \end{aligned}$$

$$\begin{aligned} &\downarrow \\ y_p &= w_{left}, \\ z_i &= t_{inf}, \\ z_s &= t_{sup}. \end{aligned}$$

3. **Third component, p_z**

Let $\zeta = \frac{(p_{y*})^2}{(y_p)^2} + \frac{(p_{z*})}{(z_i - z_s)^2} - 1$, then



After this process, the function g determined if the point (p_x, p_y, p_z) belongs to the geological body; obtaining the required information to fill our grid and a final simulation.

4 Results

In this chapter we will present some results obtained with the model developed throughout this work. In the first part, we will show the basic parameters used during the simulation of the turbidities; the results will be displayed in the second part of the chapter.

4.1 Establishing the basic parameters

Before starting the simulation, we set some initial basic data, such as the size of the grid and the domain. The values assigned to the domain depend on the range in which the parameters of turbidity are chosen; in our examples we set the domain $[-5, 5] \times [-5, 5] \times [-5, 5]$.

As we saw in figure 3.3, the grid is defined by its dimensions nx , ny , nz in the direction of each Cartesian axis respectively; thus generating a mesh $nx \times ny \times nz$ cells. In our simulation we will use a grid of $100 \times 100 \times 100$, however at the end of this chapter we will see an example where the result is observed with a grid of different sizes.

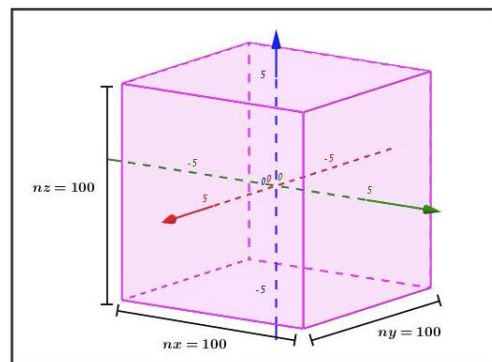


Figure 4.1: Domain and dimensions of the grid.

4.2

Simulation of turbidity

Recall that for the simulation of a turbidity different parameters are needed, which specify the final design of the body. As explained in Appendix A, our program has several values for the different data that we use, however for each example the values of the parameters of the turbidity will be given randomly such that its values are less than or equal to the information showed in the figure 5.2. For the examples that we will see in this section, the parameters that define the B-spline curves of each turbidity have the following range:

<i>Origin</i> (x, y, z)	\in	$[-5, 5] \times [-5, 5] \times [-5, 5]$
<i>w_{left}</i>	\in	$[0, 4.5]$
<i>w_{right}</i>	\in	$[0, 5.0]$
<i>length</i>	\in	$[0, 12.0]$
<i>direction</i>	\in	$[0, 360]$
<i>t_{sup}</i>	\in	$[0, 1.7]$
<i>t_{inf}</i>	\in	$[0, 1.0]$

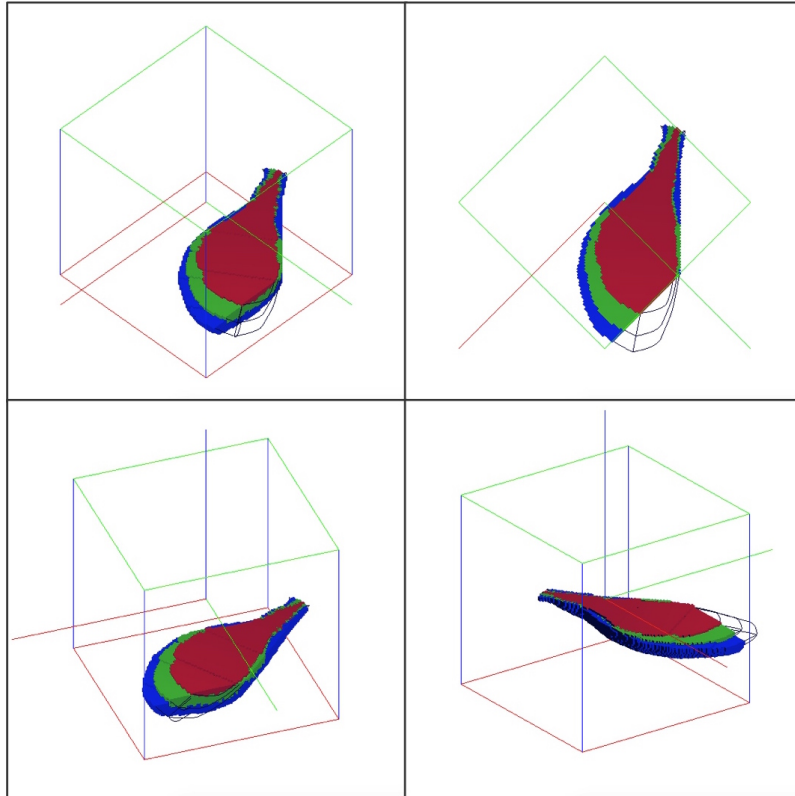
Table 4.1: Parameters of turbidity.

Now, we will see different examples of simulations varying the respective values of each of its parameters.

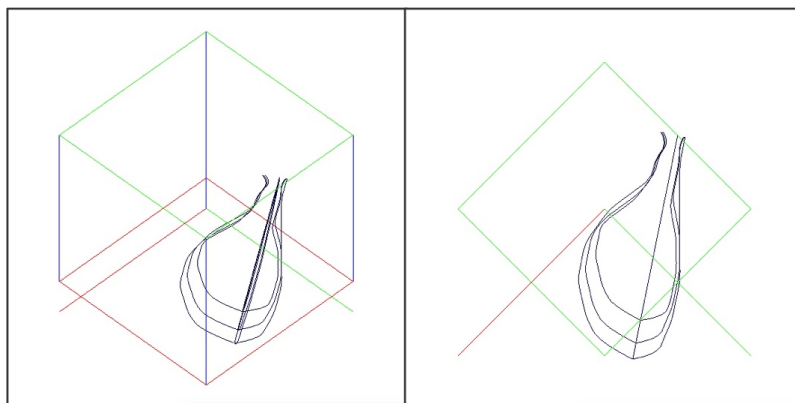
4.2.1 First simulations

In this first part we will show simulations that were considered satisfactory by its similarity to the geometric model chosen.

Example 4.2.1.1.



4.2(a): Image grid filled.



4.2(b): B-Spline curves of turbidity.

Figure 4.2: Simulation resulting turbidity, example 1.

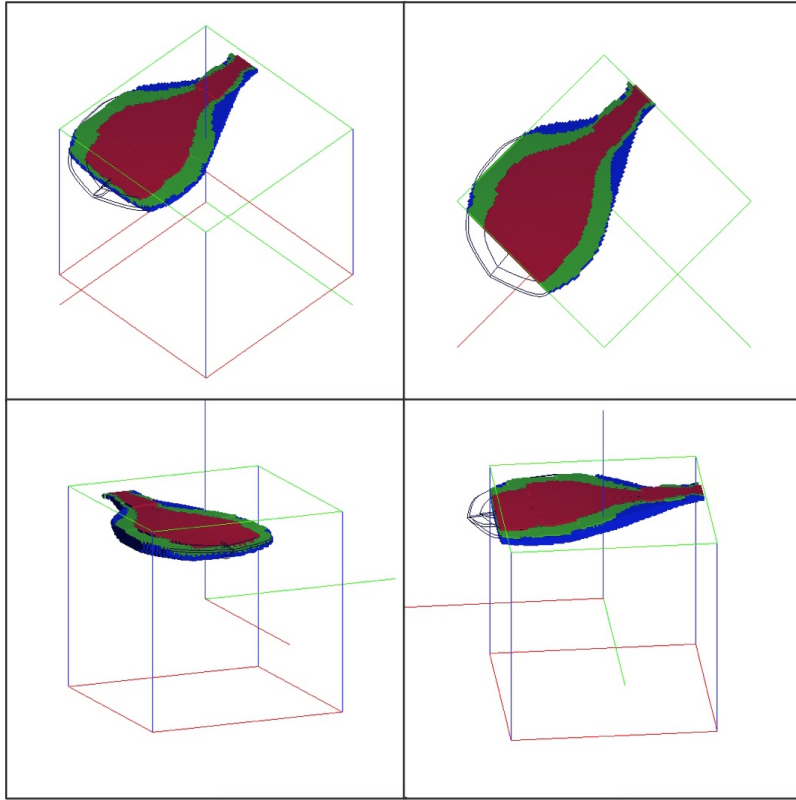
x	-4.99851
y	-0.00782025
z	-1.43499
w_{left}	3.35741
w_{right}	1.49031
$length$	10.9843
$direction$	326.387
t_{sup}	0.440337
t_{inf}	0.915078

Table 4.2: Parameters of turbidity example 1.

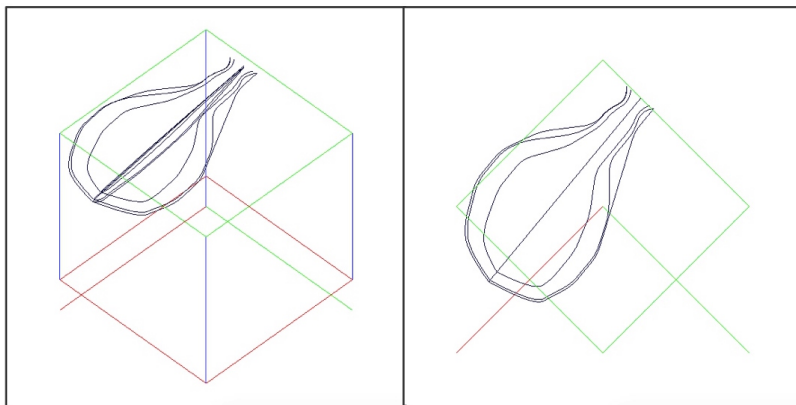
Example 4.2.1.2.

x	-4.9939
y	-2.40053
z	4.37215
w_{left}	3.59884
w_{right}	3.22338
$length$	11.5145
$direction$	354.643
t_{sup}	0.318225
t_{inf}	0.735584

Table 4.3: Parameters of turbidity example 2.



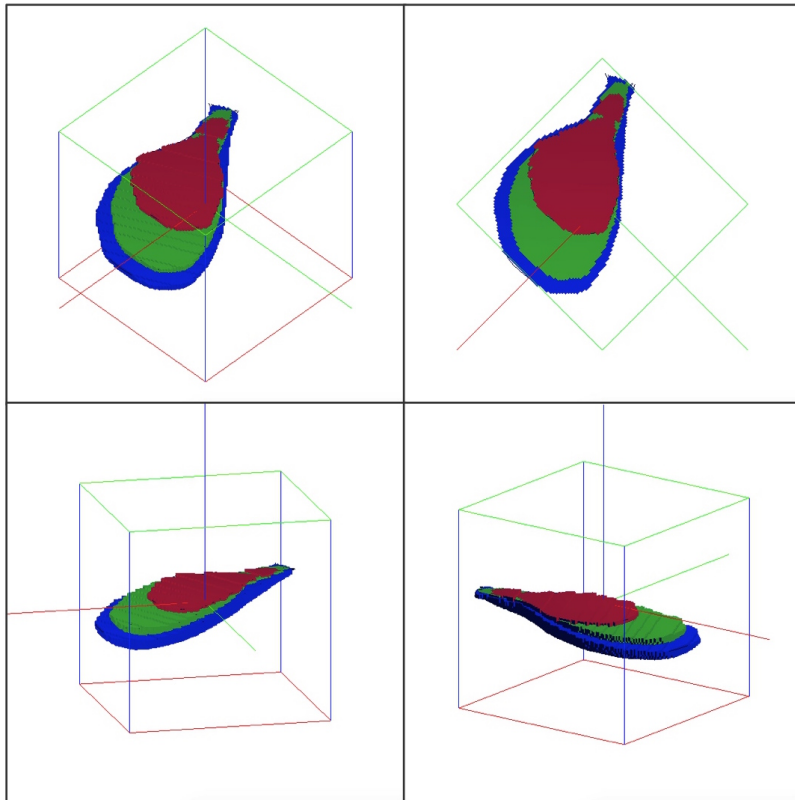
4.3(a): Image grid filled.



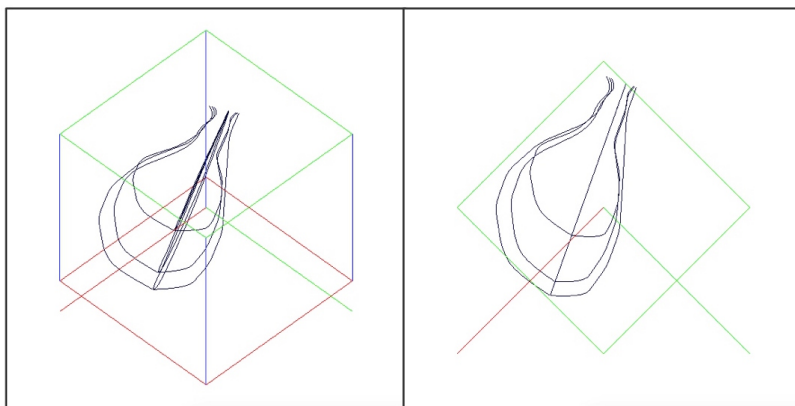
4.3(b): B-Spline curves of turbidity.

Figure 4.3: Simulation resulting turbidity, example 2.

Example 4.2.1.3.



4.4(a): Image grid filled.



4.4(b): B-Spline curves of turbidity.

Figure 4.4: Simulation resulting turbidity, example 3.

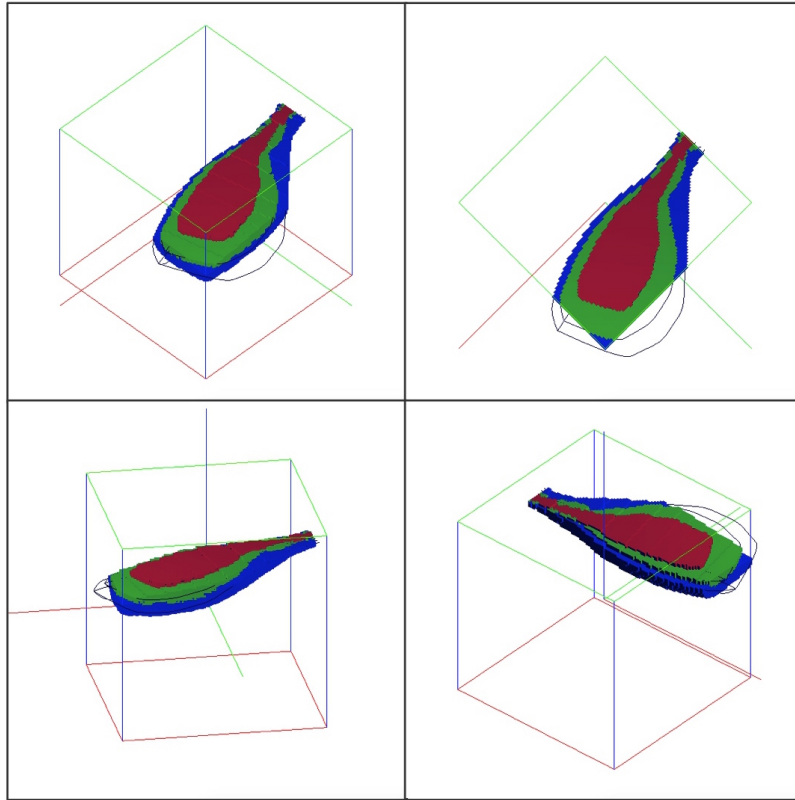
x	-4.99217
y	-3.462213
z	0.605322
w_{left}	3.96005
w_{right}	2.10689
$length$	10.8647
$direction$	334.671
t_{sup}	1.54388
t_{inf}	0.763569

Table 4.4: Parameters of turbidity example 3.

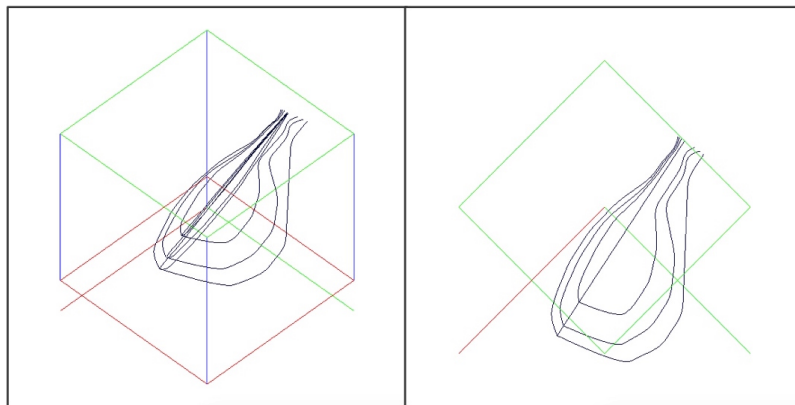
Example 4.2.1.4.

x	-4.99194
y	0.483922
z	3.27348
w_{left}	1.46385
w_{right}	4.5001
$length$	11.2307
$direction$	348.311
t_{sup}	1.02919
t_{inf}	0.876476

Table 4.5: Parameters of turbidity example 4.



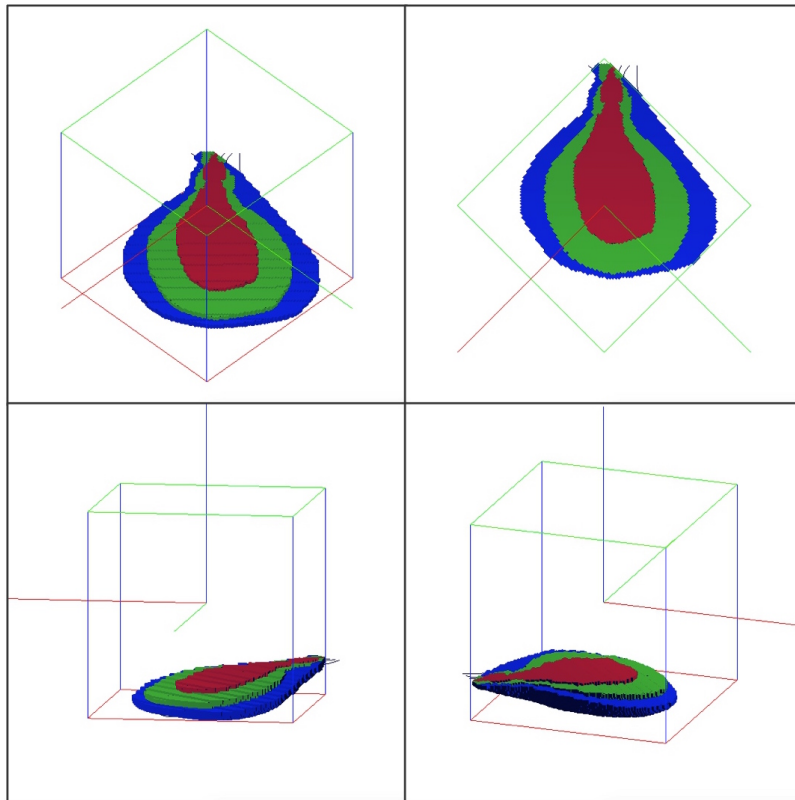
4.5(a): Image grid filled.



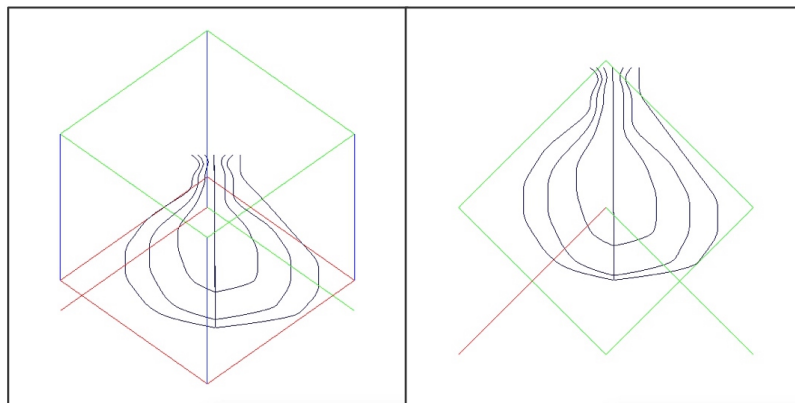
4.5(b): B-Spline curves of turbidity.

Figure 4.5: Simulation resulting turbidity, example 4.

Example 4.2.1.5.



4.6(a): Image grid filled.



4.6(b): B-Spline curves of turbidity.

Figure 4.6: Simulation resulting turbidity, example 5.

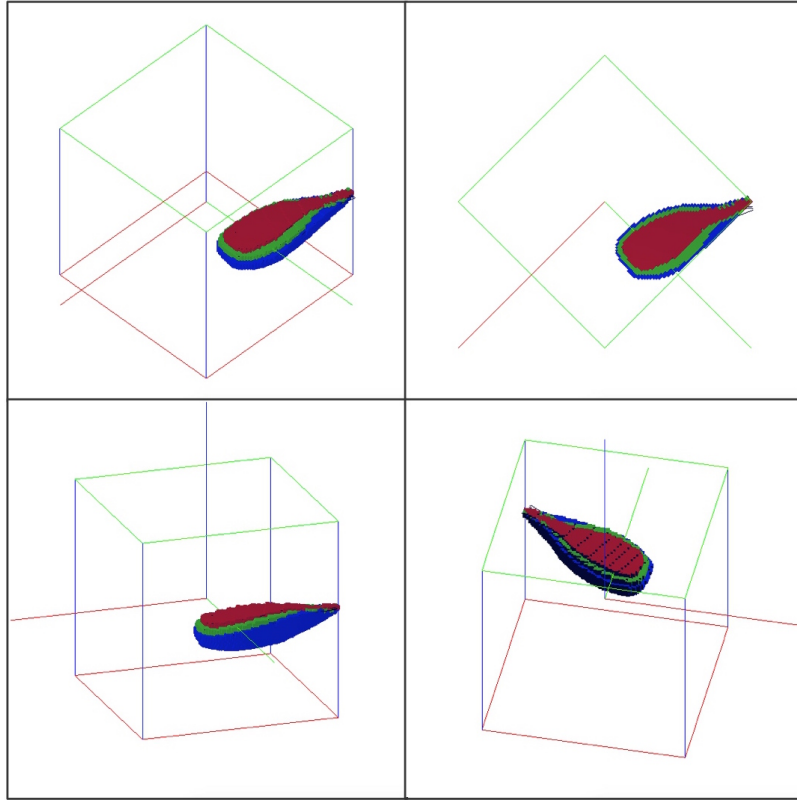
x	-4.99045
y	-4.5239
z	-3.16151
w_{left}	4.32126
w_{right}	4.99041
$length$	10.215
$direction$	314.698
t_{sup}	1.26953
t_{inf}	0.791555

Table 4.6: Parameters of turbidity example 5.

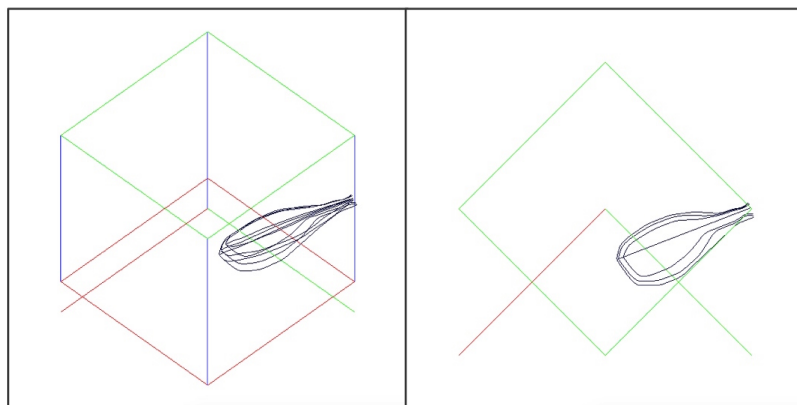
Example 4.2.1.6.

x	-4.98513
y	4.9218
z	0.650112
w_{left}	1.0741
w_{right}	1.9031
$length$	6.92148
$direction$	23.8742
t_{sup}	1.10337
t_{inf}	0.950782

Table 4.7: Parameters of turbidity example 6.



4.7(a): Image grid filled.



4.7(b): B-Spline curves of turbidity.

Figure 4.7: Simulation resulting turbidity, example 6.

4.2.2 Simulations with difficulties

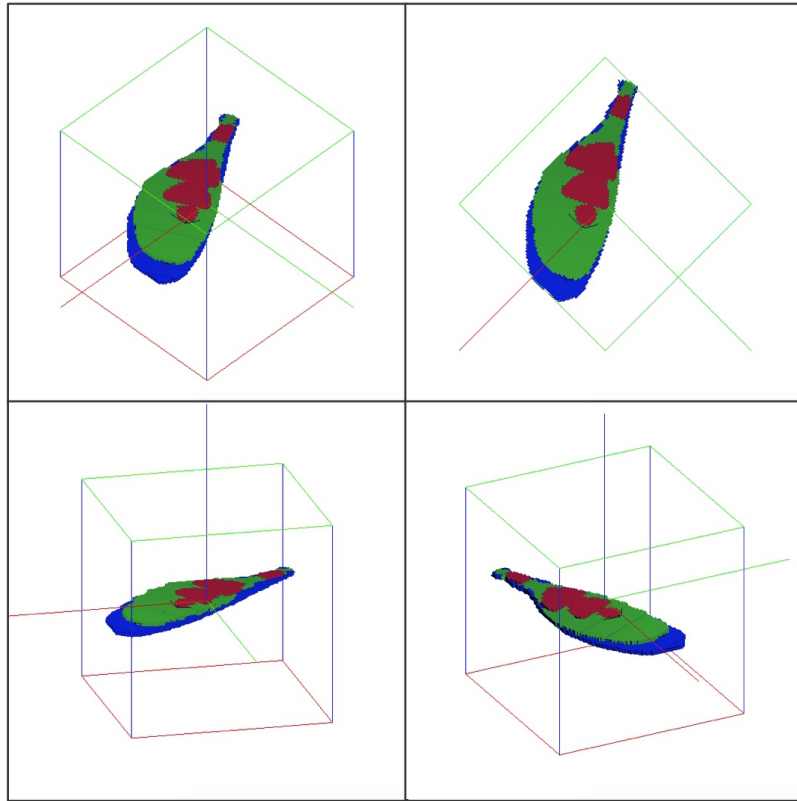
In the second part of the results of simulations, we discuss some cases that can not be as faithful to the chosen geometric pattern, this is because the parameters of each of the examples is randomly generated.

Example 4.2.2.1.

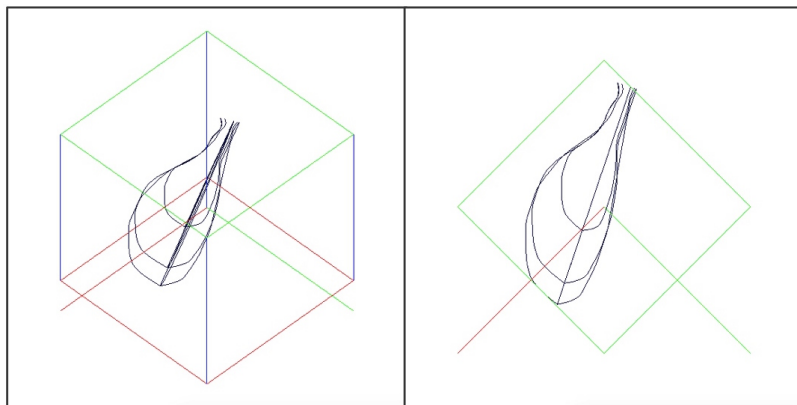
In this example we see that the upper lobe of turbidity has "holes" on the surface; this is because the thickness t_{inf} of the turbidity is small and to simulate the B-Spline curves associated with t_{inf} for each of the lobes, these reduce even more the value of this parameter; such that the resulting image to generate in the grid, the cells corresponding to this lobe are not filled as belonging to the geological body.

x	-4.99632
y	-3.17724
z	0.134501
w_{left}	2.72622
w_{right}	1.16024
$length$	11.0664
$direction$	333.695
t_{sup}	0.636623
t_{inf}	0.368878

Table 4.8: Parameters of turbidity example 1.



4.8(a): Image grid filled.

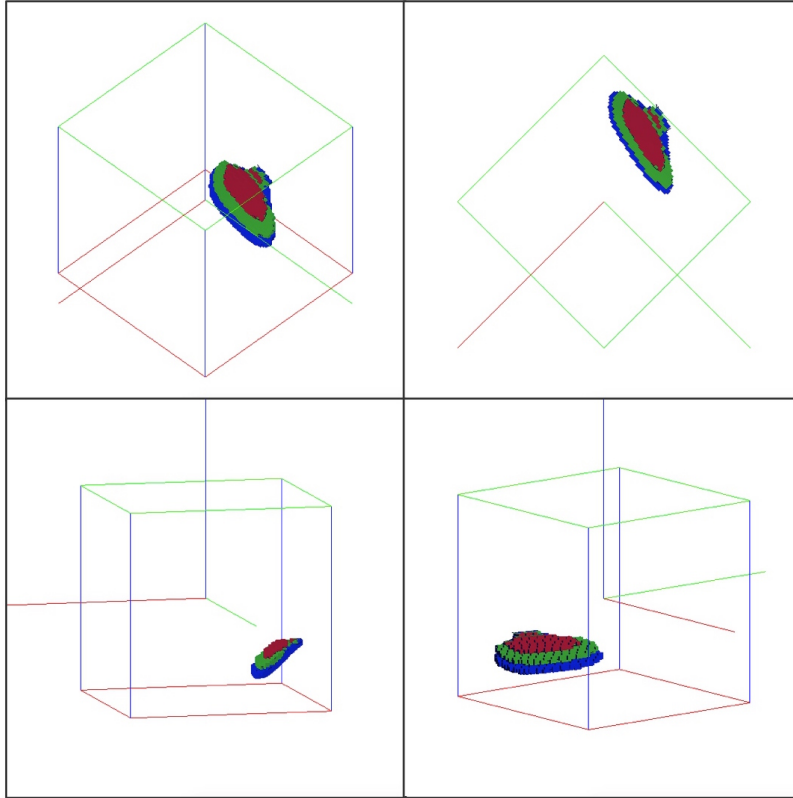


4.8(b): B-Spline curves of turbidity.

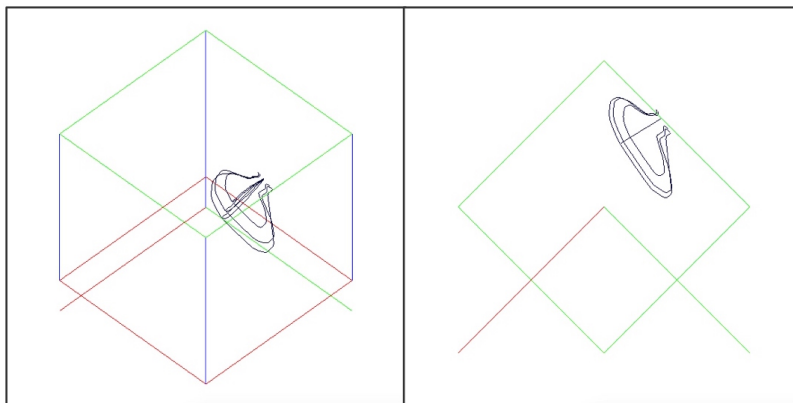
Figure 4.8: Simulation resulting turbidity, example 1.

Example 4.2.2.2.

In this second example we can observe a turbidity with small length, and therefore the simulated object has neither the length nor the desired shape.



4.9(a): Image grid filled.



4.9(b): B-Spline curves of turbidity.

Figure 4.9: Simulation resulting turbidity, example 2.

x	-4.99977
y	-1.05387
z	-2.33184
w_{left}	2.0038
w_{right}	3.39321
$length$	2.36594
$direction$	13.6401
t_{sup}	1.18532
t_{inf}	0.312907

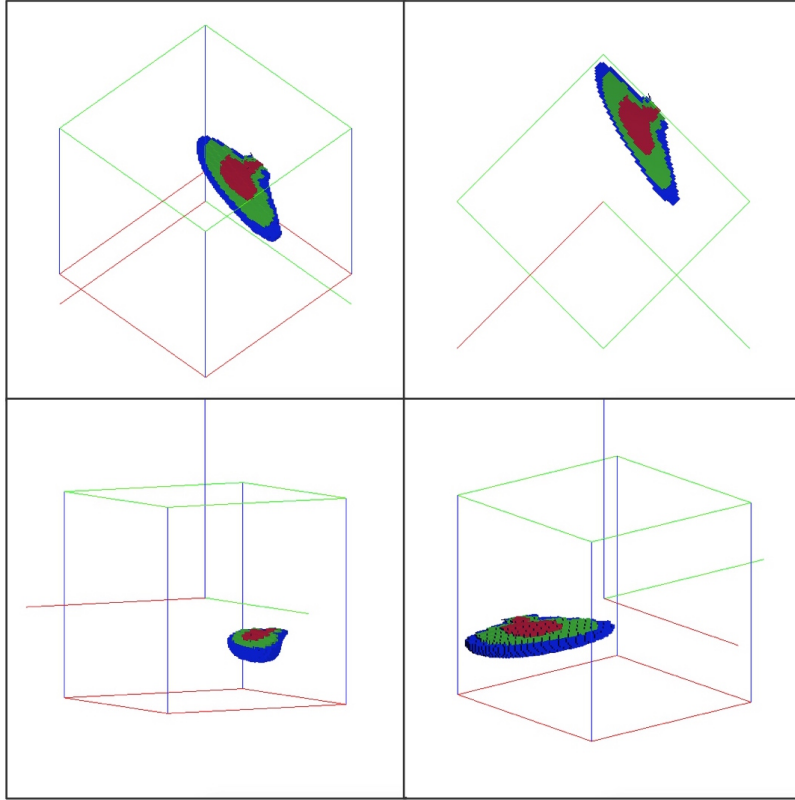
Table 4.9: Parameters of turbidity example 2.

Example 4.2.2.3.

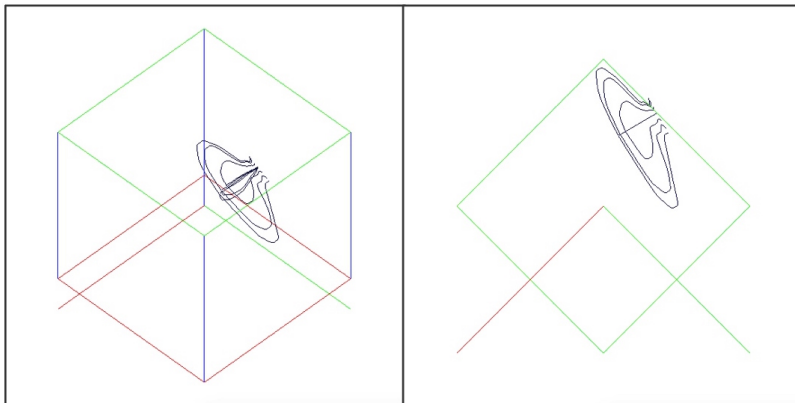
Like the previous example this turbidity has low length, also the values obtained for their parameters w_{right} and w_{left} are significantly higher than the total length; getting the body obtained has a oblate shape on their sides.

x	-4.99562
y	-1.33884
z	-1.86102
w_{left}	3.23763
w_{right}	4.33986
$length$	2.16424
$direction$	14.6155
t_{sup}	0.592572
t_{inf}	0.707599

Table 4.10: Parameters of turbidity example 3.



4.10(a): Image grid filled.

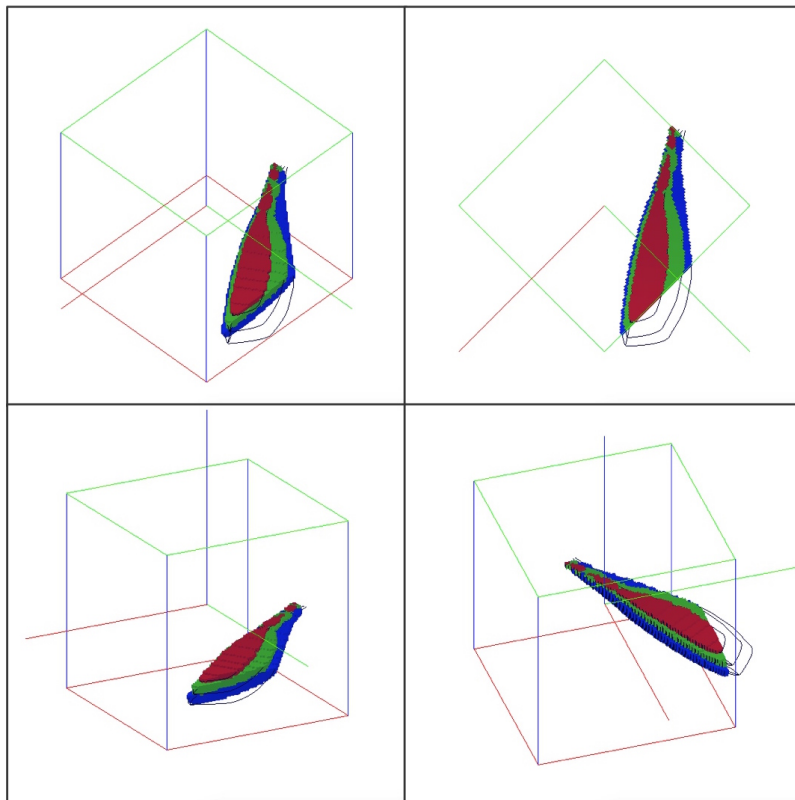


4.10(b): B-Spline curves of turbidity.

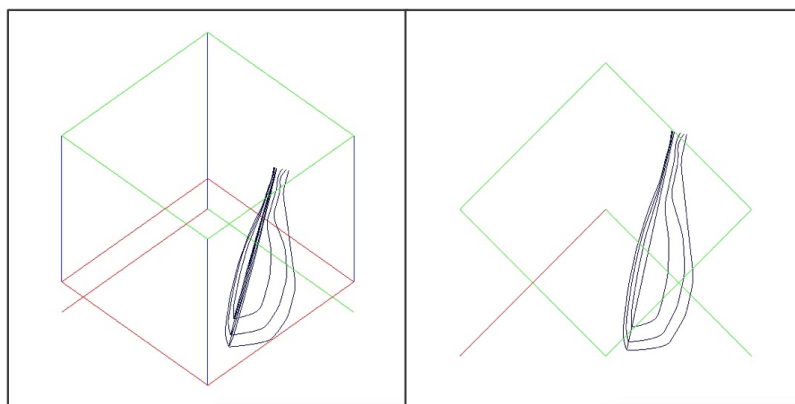
Figure 4.10: Simulation resulting turbidity, example 3.

Example 4.2.2.4.

In our work has been given freedom among the parameters that determine the width (both right and left) of turbidity and the resulting model is not symmetrical, for that reason, to obtain random values w_{right} and w_{left} , it is possible to occur the case that one of them is considerably higher than the other; thus resulting in a geological body with little resemblance to the original model.



4.11(a): Image grid filled.



4.11(b): B-Spline curves of turbidity.

Figure 4.11: Simulation resulting turbidity, example 4.

x	-4.99437
y	-0.292793
z	-0.964168
w_{left}	0.591238
w_{right}	2.43696
$length$	10.7826
$direction$	327.363
t_{sup}	1.34759
t_{inf}	0.50977

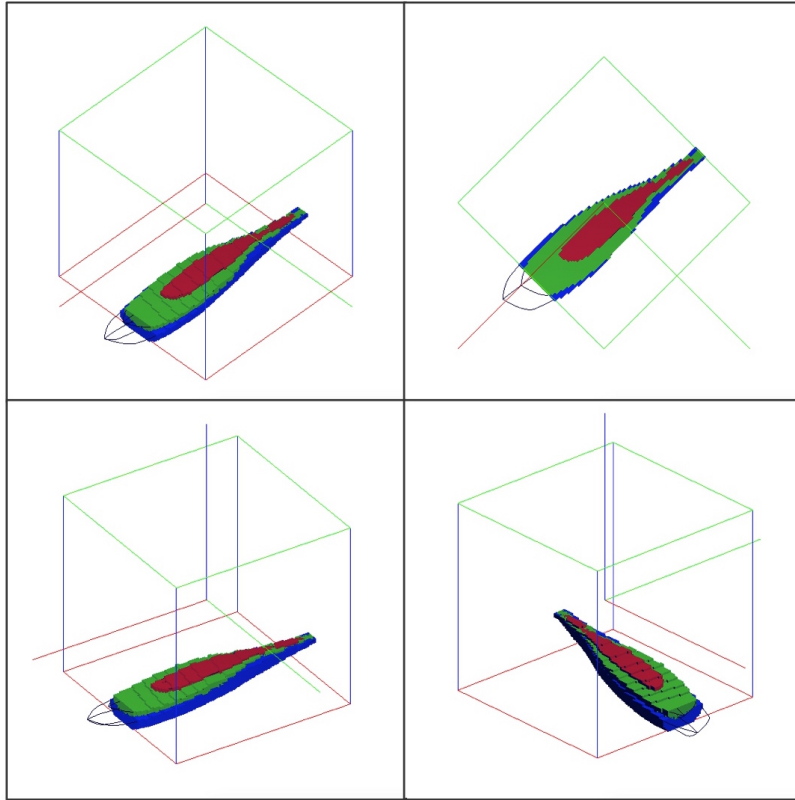
Table 4.11: Parameters of turbidity example 4.

Example 4.2.2.5.

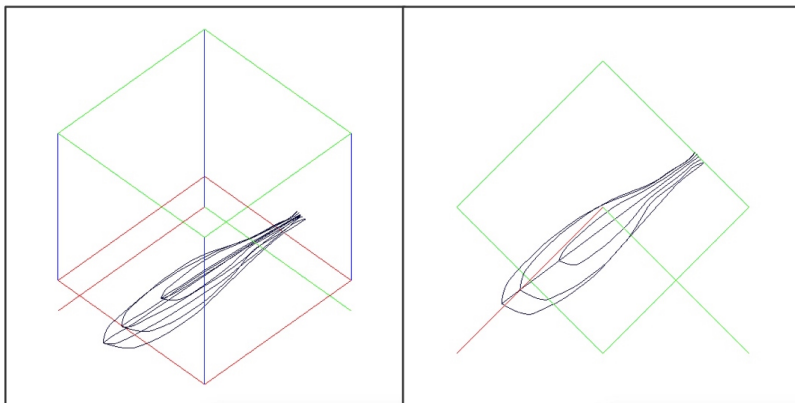
In this case, we observe an elongated turbidity, this is because its length is large with respect to their widths.

x	-4.99366
y	1.54561
z	-2.95969
w_{left}	1.10264
w_{right}	1.61658
$length$	11.8804
$direction$	8.28319
t_{sup}	1.30354
t_{inf}	0.848491

Table 4.12: Parameters of turbidity example 5.



4.12(a): Image grid filled.



4.12(b): B-Spline curves of turbidity.

Figure 4.12: Simulation resulting turbidity, example 5.

Example 4.2.2.6.

In this last example an object outside the grid was obtained; although its origin is within the mesh as the design also depends on other parameters such as direction, length, it can submit the resulting geological body is outside the domain.

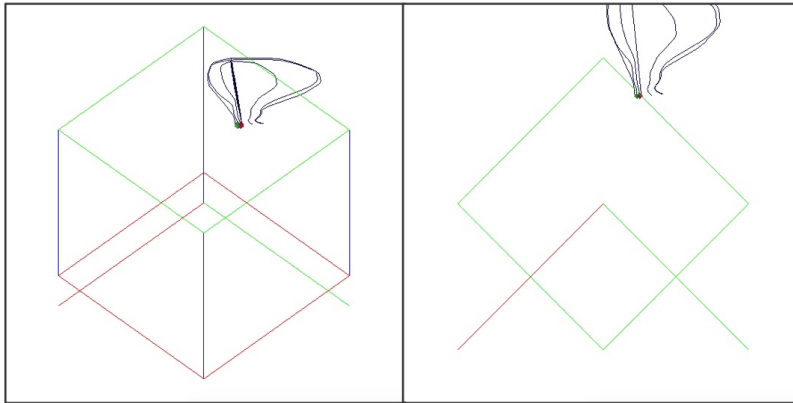


Figure 4.13: Simulation resulting turbidity, example 6.

x	-4.99984
y	-2.36924
z	0.112106
w_{left}	4.1692
w_{right}	1.26214
$length$	5.57729
$direction$	129.093
t_{sup}	0.856878
t_{inf}	0.275271

Table 4.13: Parameters of turbidity example 6.

5 Conclusion

During the development of this project we have addressed the object modelling turbidity lobes; these have been studied as three-dimensional bodies to abstracting an overall characteristics of its form and try to produce a result that can be adjusted to our needs and interests, both in width and thickness.

5.1 Conclusions of the project

As explained throughout the development of this work, our model is a simple turbidity which has three lobes; This will be generated with random parameters obtained but at the same time they are restricted to a range established so that the result is as close as possible to design taken as our conceptual model. Although we determine the ranges for each parameter according to our model, these can be adjusted according to the characteristics required of each object selected.

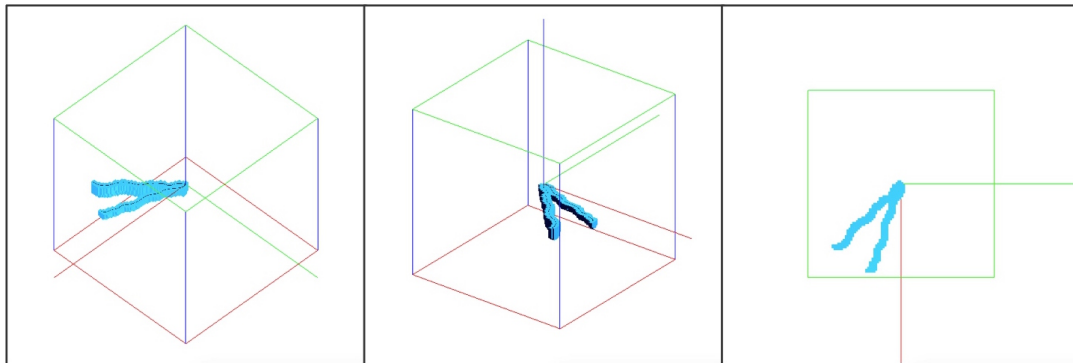
On completion of this project we can offer results in a depositional model, whose contour is designed by B-Spline curves. This system was built with three lobes to facilitate the process, but can be extended to a larger number of lobes without any difficulty.

Finally, the choice independently of the parameters to provide the width (right and left) and thickness (upper and lower) gives us the ability to see patterns that are not necessarily symmetrical and getting more realistic results.

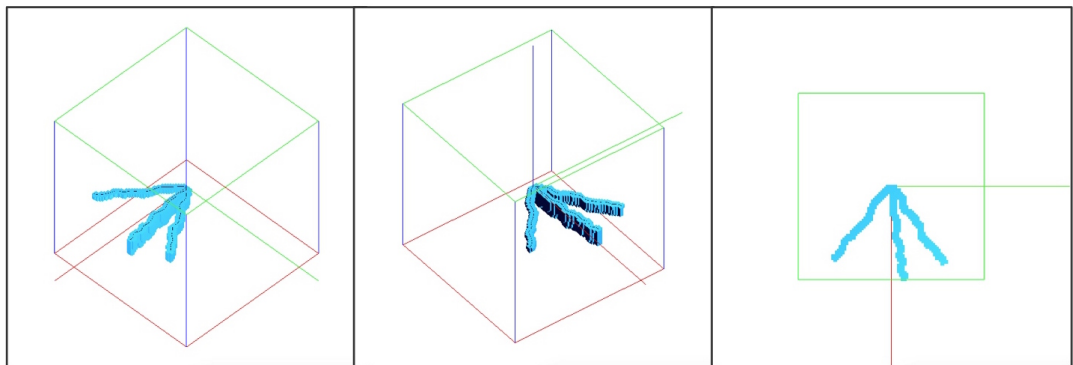
5.2

Future works

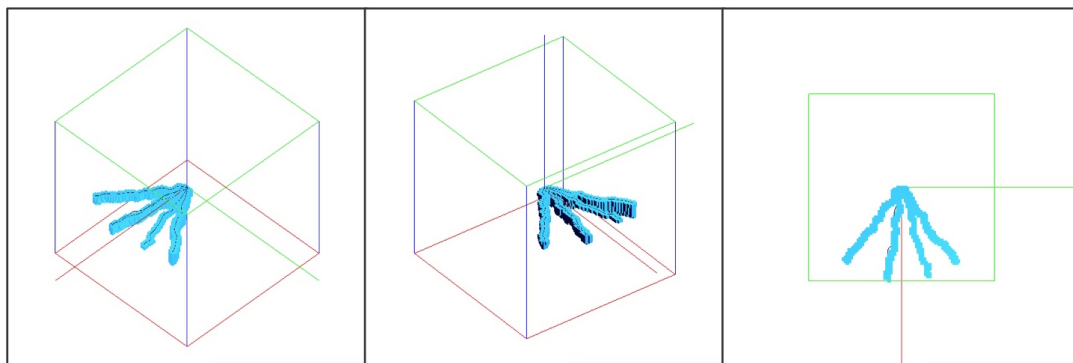
At the conclusion of the work of modelling of turbidity lobes, immediately arises interest in modelling possible channels inside these geological bodies. Based on research conducted in “*Object-Based Modeling of Fluvial Reservoirs*” (Sanabria, 2016) we can try to link both models simulations to determine the channels according to the parameters of turbidity and develop a series of branched channels within turbidity lobes. In image 5.1 we see some examples of channels that have equal length and origin, these channels were obtained with the Master Dissertation “*Object-Based Modeling of Fluvial Reservoirs*” (Sanabria, 2016). To improve the simulation time, we observe that the *in_out* operation can be doing using parallel processing.



5.1(a): 2-channel simulation.



5.1(b): 3-channel simulation.



5.1(c): 4-channel simulation.

Figure 5.1: Simulation of channels with the same origin and bounded length.

Bibliography

BARRETO, A., FARIAS, R., KRUEL, R., LANZARINI, W., LOPES, H., PESCO, S., AND TAVARES, G. 1995. Petbool: simulador estocástico da geometria e heterogeneidades de reservatórios petrolíferos usando o método booleano. In *Primeiro Workshop em Simulação e Engenharia de Reservatórios*, pages 26–27.

BISCHOFF, A., SOARES, A., LAYAN, C., CORREIA, G., AND PINHEIRO, J. 2007. Processos e fácies em turbiditos. Trabalho final do curso de especialização em projeto de análise de bacias, módulo geologia do petróleo, Universidade do Estado do Rio de Janeiro, Faculdade de Geologia.

DEUTSCH, C. AND PYRCZ, M. 2014. *Geostatistical Reservoir modeling*. Oxford University Press, second edition.

DEUTSCH, C. AND TRAN, T. 2002. FLUVSIM: a program for object-based stochastic modeling of fluvial depositional systems. *Computers and Geosciences*, 28(4):525–535.

DEUTSCH, C. AND WANG, L. 1996. Hierarchical object-based stochastic modeling of fluvial reservoirs. *Mathematical Geology*, 28(7):857–880.

FARIN, G. 1997. *Curves and Surfaces for Computer-Aided Geometric Design: A Practical Code*. Academic Press Inc., fourth edition.

FARIN, G. 2002. *Curves and Surfaces for CAGD. A practical guide*. Morgan Kaufmann Publishers Inc., fifth edition.

FREITAS, V. 2004. Estratigrafia e sistema deposicional dos complexos de canais turbidíticos ainsa I e II, Centro Sul dos Pirineus, Espanha. Universidade do Estado de Rio de Janeiro. Faculdade de Geologia. Departamento de Estratigrafia e Paleontologia (DEPA).

MARIETHOZ, G. AND CAERS, J. 2015. *Multiple-point geostatistics: Stochastic modeling with training images*. Wiley Blackwell.

MUTI, E., TINTERRI, R., REMACHA, E., MAVILLA, N., ANGELLA, S., AND FAVA, L. 2002. *An Introduction to the Analysis of Ancient Turbidite Basins from an Outcrop Perspective*. The American Association of Petroleum Geologists, second edition.

MÄNTYLÄ, M. 1988. *An Introduction to solid Modeling*. Computer Science Press.

NEUENDORF, K. 2005. *Geology Glossary*. Springer Science & Business Media, fifth edition.

PAIM, P., FACCINI, U., AND NETTO, R. 2003. *Geometria, arquitetura e heterogeneidades de corpos sedimentares*. Universidade do Vale do Rio dos Sinos - UNISINOS.

PESSINI, S. 2013. Simulação estocástica baseada em objetos: Aplicação aos depósitos turbidíticos do campo escola de namorado. Master's thesis, Universidade de São Paulo. Instituto de Geociencias, Programa de Pos-Graduação em Recursos Minerais e Hidrogeologia.

PHAN, V. 2002. *Modeling Technique for Generating Fluvial Reservoir Descriptions Conditioned to Static and Dynamic Data*. PhD thesis, Stanford University.

PIEGL, L. AND TILLER, W. 1996. *The NURBS Book*. Springer-Verlag, second edition.

PRAUTZSCH, H., BOEHM, W., AND PALUSZNY, M. 2002. *Bézier and B-Spline Techniques*. Springer-Verlag Berlin Heidelberg.

ROSELL, J. 1989. LÃmites en series turbidÃncas. *Revista de la Sociedad GeolÃgica de EspaÃsa*, (2):375–380.

SALOMON, D. 2006. *Curves and Surfaces for Computer Graphics*. Springer Science+Business Media Inc.

SANABRIA, R. 2016. Object-based modeling of fluvial reservoirs. Master's thesis, Pontifícia Universidade Católica do Rio de Janeiro.

SÁNCHEZ-REYES, J. 1994. Single-valued tubular patches. *Computer Aided Geometric Desing*, 11(5):565–592.

SANTOS, G., LOPES, H., PESCO, S., AND POLETTI, C. 2002. Petbool: a software for stochastic modeling of geological objects. In *TERRA NOSTRA Series, Proceeding of the Mathematical Geology'02*, pages 179–184. IAMG, Berlim, 1 edition.

Appendix A

Program parameters

The parameters of our turbidity model are described in figure 5.2, which is made to design bodies with adequate geometry parameters presented above. It is not an optimal program for speed. However, it may be useful for simulating and sketching possible bodies of interest in research in this area. The parameters required for the program are listed below and a parameter file is shown in the figure 5.2:

- Line 1: domain of the x coordinate.
- Line 2: domain of the y coordinate.
- Line 3: domain of the z coordinate.
- Line 4: the size of the model in the x, y, z directions.
- Line 5: number of embodiments of generating.
- Line 6: maximum number of lobes to generate.
- Line 7: vector with geometrical specification of all objects turbidity. This vector is used to store the characteristics of each lobe.
- Line 8: number of lobes to be made.
- Line 9: overall proportions of width and thickness of each lobe over the previous.
- Line 10: *width left* turbidity B-Spline curve.
- Line 11: parameter matrix for the *width left* curve.
- Line 12: *width right* turbidity B-Spline curve.
- Line 13: parameter matrix for the *width right* curve.
- Line 14: *thickness sup* turbidity B-Spline curve.
- Line 15: parametrization matrix *thickness sup* curve.

- Line 16: *thickness inf* turbidity B-Spline curve.
- Line 17: parametrization matrix *thickness inf* curve.
- Line 18: the lobe corresponding level.
- Line 19: width parameter ratio to model the turbidity lobe of the next level. The first lobe ratio is 1 with respect to turbidity.
- Line 20: thickness ratio parameter to model the turbidity lobe of the next level. The first lobe ratio is 1 with respect to turbidity.
- Line 21: turbidity origin of coordinates.
- Line 22: horizontal length to *width left* of turbidity.
- Line 23: horizontal length to *width right* of turbidity.
- Line 24: total length of turbidity in the x direction.
- Line 25: turbidity orientation angle measured in degrees clockwise. Is output from the centreline of turbidity representing the central axis of the body.
- Line 26: vertical length to *thickness sup* of turbidity.
- Line 27: vertical length to *thickness inf* of turbidity..
- Line 27: total number of lobes to simulate this turbidity.
- Line 29: scale width of each lobe compared to the previous.
- Line 30: scale thickness of each lobe compared to the previous.

Line 1	Domain x : coordinates x_{min}, x_{max}	-5.0	5.0
Line 2	Domain y : coordinates y_{min}, y_{max}	-5.0	5.0
Line 3	Domain z : coordinates z_{min}, z_{max}	-5.0	5.0
Line 4	Grid size: n_x, n_y, n_z	100	100 100
Line 5	Number of embodiments to generate	1	
Line 6	Number of lobes to generate	3	
Line 7	Vector for simulation turbidity	$V_{tb}(11.0, 0.0)$	
Line 8	Upper lobe, middle lobe, lower lobe	1	1 1
Line 9	Proportion: turbidites, lobes	1	1
Line 10	B-Spline curve <i>width left</i>	B-Spline	w_{left}
Line 11	Matrix numbers	$M[14][3]$	
Line 12	B-Spline curve <i>width right</i>	B-Spline	w_{right}
Line 13	Matrix numbers	$M[14][3]$	
Line 14	B-Spline curve <i>thickness sup</i>	B-Spline	t_{sup}
Line 15	Matrix numbers	$M[14][3]$	
Line 16	B-Spline curve <i>thickness inf</i>	B-Spline	t_{inf}
Line 17	Matrix numbers	$M[14][3]$	
Line 18	Turbidity: level lobe	1	2 3
Line 19	Turbidity: width ratio parameter	1	
Line 20	Turbidity: thickness ratio parameter	1	
Line 21	Turbidity: point of origin	0	0 0
Line 22	Turbidity: width left	4.5	
Line 23	Turbidity: width right	5.0	
Line 24	Turbidity: length	12.0	
Line 25	Turbidity: direction	$RAND - MAX$	
Line 26	Turbidity: thickness sup	1.7	
Line 27	Turbidity: thickness inf	1.0	
Line 28	Lobes: number of lobes	3	
Line 29	Lobes: width scale	1	
Line 30	Lobes: thickness scale	1	

Figure 5.2: Parameter file.